The development of a plastic scintillator for radiotherapy dosimetry

Johnny Estuardo Morales
University of Wollongong

THE DEVELOPMENT OF A PLASTIC SCINTILLATOR FOR RADIOTHERAPY DOSIMETRY

A thesis submitted in fulfilment of the

requirements for the award of the degree

Master of Science By Research

from

UNIVERSITY OF WOLLONGONG

by

Johnny Estuardo Morales

BMedPhys(Hons)

Department of Engineering Physics

2008

CERTIFICATION

I, Johnny Estuardo Morales, declare that this thesis, submitted in fulfilment of the requirements for the award of Master of Science, in the Department of Engineering Physics, University of Wollongong, NSW, Australia is wholly my own work unless otherwise referenced or acknowledged. The document has not been submitted for qualifications at any other academic institution.

Johnny E. Morales

19th March 2008

TABLE OF CONTENTS

LIST OF TABLES

LIST OF FIGURES

ABSTRACT

A plastic scintillator detector was developed and tested in a 6MV photon beam. The detector comprised a BCF60 plastic scintillator, Polymetyl-Methacrylate Resin optical fibre and photodiode SFH250. The detector was used to measure an inplane profile for the photon beam at a depth of 1.5 cm for a field size of 10x10cm^2 at 100 cm SSD. The photon beam was delivered by a Siemens linear accelerator. A comparison was made with the results obtained by cylindrical chambers CC04 and CC13, commercial diode PFD and a stereotactic diode SFD, all from the manufacturer IBA-Wellhöfer. An analysis was performed using the Gamma Evaluation method and the agreement was acceptable for a criterion of Distance To Agreement = 2 mm and Dose Difference = 2%.

ACKNOWLEDGMENTS

I would like to acknowledge the help I have received from my main supervisor Associate Professor Bill Zealey from the Department of Engineering Physics at the University of Wollongong, NSW, Australia. He has given me guidance and advice on the project and I am very thankful to him. His final push for completion helped me to get over the line. Thanks a lot Bill.

I also acknowledge the assistance I received from Mr. Nigel Freeman, Chief Physicist at St Vincent's Hospital in Sydney, Australia while I was employed by him and during the measurements presented in this thesis. Nigel's vision and sound advice are greatly appreciated.

I would like to thank Dr. Mamoon Haque, Senior Physicist at Royal Prince Alfred Hospital in Sydney, who provided plenty of advice and positive criticism. His valuable advice was tremendous. And I appreciate his promptness and readiness to assist. His higher degree experience and his medical physics experience were extremely valuable.

I would like to acknowledge Dr Sue Law from The University of Sydney for her assistance in coupling the Silica Fibre to the photodiode.

I also would like to acknowledge Dr Anatoly Rozenfeld from the University of Wollongong for his initial encouragement at the beginning of this project.

Finally, I would like to acknowledge my family for their endless support and above all for their infinite encouragement. My family was always there for me at all times and their genuine support has always been a source of motivation for this project, for my personal life and for my professional development in my chosen career as a medical physicist.

C h a p t e r 1

Introduction: dosimetry in radiotherapy

1.1 Introduction

Radiotherapy involves the treatment of cancer patients with high energy x–ray and electrons beams. Dosimetry is a fundamental field in radiotherapy that requires high standards of equipment and technique in order to achieve excellence in patient care. As a consequence the medical physicist investigates and researches new materials and techniques to improve existing methods in dosimetry.

One area of radiotherapy dosimetry which has been the target of exhaustive investigation is plastic scintillator dosimetry. The work presented in this thesis deals with the development of plastic scintillator dosimetry and its application in radiotherapy.

1.2 Objectives and Brief Description of Current research

1.2.1 Objectives

The main objective of the research presented in this thesis was

- to develop a dosimetry system comprised of: a plastic scintillator, optical fibre and a photodiode.
- to compare the performance of this system against existing detectors that are in common use in radiotherapy.

1.2.2 Brief Description

Through study and research of the literature a strategy was formulated to create a plan that would enable the development of a plastic scintillator system that made use of single optical fibre as the signal conducting medium from a plastic scintillator to a photodiode. However, due to technical hurdles this was not possible and a new approach was adopted. The new approach involved the use of a commercially available photodiode designed for the telecommunication industry and the design of a plastic scintillator-to-optical fibre coupling technique.

1.3 Thesis Outline

This thesis follows this structure:

Chapter 1 is a very brief introduction and description of the research conducted and its objectives. A summary of current dosimetry in radiotherapy is presented. This is followed by a short discussion on the advantages and disadvantages of plastic scintillators and optical fibres in radiotherapy.

Chapter 2 presents the theoretical physics background on plastic scintillators and optical fibres. A brief literature review is presented which includes the work published by other physicists at the time that the experiments in this thesis were performed. A description on the ideal system is discussed. Another short discussion on the work published after the experiments in this thesis were performed.

Chapter 3 is dedicated to the technique of coupling the different components that comprised the plastic scintillator detector. The couplings included plastic scintillator to optical fibre and that of optical fibre to photodiode. The final design used in the experiments is described.

Chapter 4 presents the method used to do the measurements using commercial ion chambers and commercial diodes plus the results obtained with the plastic scintillator. To compare all results obtained the Gamma Evaluation method was used. A discussion of this method is presented. And an analysis based on this method is presented.

Chapter 5 is a conclusion and discussion on the achieved objectives for this project.

1.4 Existing Dosimetry in Radiotherapy

Radiotherapy involves the treatment of cancer with high energy x-rays and electrons. Excellence in patient care demands high standards of dosimetry. In order to achieve high quality, appropriate instrumentation is required. At present some of the common dosimeters which are used include ionisation chambers, film, TLDs, diodes, mosfets, diamond detectors and gel. The following section briefly describes these detectors as used in radiotherapy and their advantages and disadvantages.

1.4.1 Ionisation Chambers

The two most frequently used ionisation chambers (Metcalfe et al 1997) in radiotherapy departments are the cylindrical thimble type and the plane parallel or parallel plate. There is an extensive source of information about their design, radiation properties as well as historical advancement in their application in radiation oncology (Khan 1984, Attix 1986, Johns and Cunningham 1983, Metcalfe 1997).

1.4.1.1 Cylindrical Ionisation Chambers

A commonly used cylindrical chamber is the Farmer-type chamber. This chamber was originally designed by Farmer in 1955 (Khan 1984). It was later modified by Aird and Farmer (Khan 1984) to improve the energy response characteristics and refine the constancy of the design. See figure 1.1 for a diagram of this chamber.

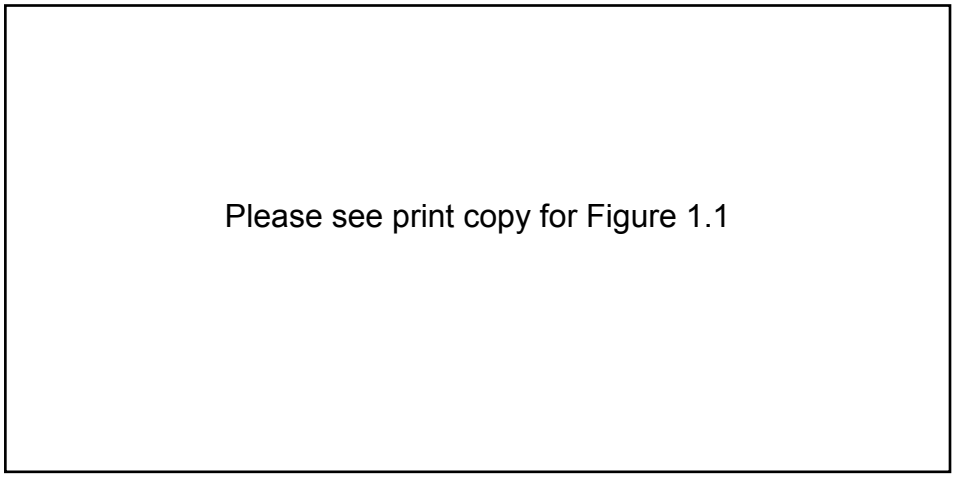

Figure 1.1 Farmer chamber. Reproduced from The Physics of Radiation Therapy by F. M. Khan

As shown a typical Farmer-type chamber has an inner electrode made from aluminium. The inner radius of the outer electrode is approximately 6.25 mm and the length of the air cavity is approximately 21.4 mm in length. Most Farmer chambers have a graphite wall but some have a plastic wall. The nominal collecting volume of this chamber is 0.6 cm^3.

Farmer Type chambers – Mode of operation

This chamber has three electrodes. A central electrode, the thimble wall and the guard electrode. The central electrode collects the current produced in the gas cavity by the radiation. This current delivers a charge to the electrometer. The thimble is held at ground potential and the guard electrode is held the same bias voltage as the collector electrode. The purpose of the guard electrode is to prevent leakage current from the collector electrode. The electrometer to which the chamber is connected provides a high bias voltage, typically 300V, on the collector electrode. Electrometers are capable of providing either positive or negative polarity to enable the measurement of polarity effects. This high voltage potential is usually variable to allow the measurement of recombination effects through the two-voltage method (IAEA-TRS398).

Farmer Type chambers – Advantages and Disadvantages

Since their invention these chambers have shown many positive advantages, such as:

- Flat energy response over the therapeutic range in radiotherapy.

- High reproducibility and accuracy when tested against Strontium 90 gamma sources

- Suitable for routine Quality Assurance tests as frequently performed in radiotherapy departments

- Ease of fabrication enabling mass production of these chambers by different manufacturing companies with excellent reproducibility

- They have become the gold standard ion chamber in radiotherapy for absolute calibration by many Secondary Standard laboratories around the world

- International bodies such as IAEA have based their protocols for Co-60 and photon beam on these chambers

There may be some disadvantages for these chambers including:

- brittleness of graphite wall which requires handling with maximum care as accidental drops or hits may crack the wall and render the chamber unreliable

- non-linear response for very low energy photon beams below HVL 1.0 mm Al

- high perturbation effects for electron beams below 10 MeV energy. For these electron energies other type of ion chambers are recommended.

1.4.1.2 Parallel Plate Ionisation Chambers

Parallel plate chambers are recommended for electron beam dosimetry by International Protocols (IAEA, NACP, AAPM, SEFM). In specific terms, for measurements in electron beams where Eo = 10 MeV parallel plate chambers are recommended, but below Eo = 5 MeV these chambers are a must (IAEA-TRS381).

As the name implies this chamber consists of two circular plates parallel to each other. The first plate is a thin foil of graphite material and it has a recommended thickness of 1 mm (IAEA 381). The second plate is another electrode which is surrounded by a guard ring structure. The separation gap between both plates is between 1 to 2 mm. The effective point of measurement for these type of ion chambers is on the inner surface of the first plate. There are a number of different designs for this type of chamber. Some of them include the Markus chamber, the NACP chamber, the Roos chamber, the Attix chamber.

Parallel plate chambers- Advantages and Disadvantages

The positive advantages for these chambers include:

- their suitable application in electron beam dosimetry in minimising the perturbation effects through their narrow electrode gap
- minimisation of the electron in-scattering effect by having a guard ring structure
- they have been adopted as the optimum chamber for electron beam dosimetry in the low energy range

Some disadvantages include:

- brittleness and fragility of front window which requires extreme care from user
- readings obtained through electrometers represent the ionisation in the cavity and not the absorbed dose therefore other correction factors are applied to convert to absorbed dose measurement
- they require environmental corrections including temperature and pressure correction

1.4.1.3 Film

1.4.1.3.1 Radiographic Emulsions

Film is also used for dosimetry in photon and electron beams. Major use is for QA of Linac etc. (Wang et al 2005). Unique in providing simultaneous 2-D dose maps

In fact film was the detector which was originally used in the discovery of x-rays. Film is available as single emulsion or double emulsion. Single emulsion type has a transparent film base of about 0.2 mm coated with emulsion on one side only. The base is usually either cellulose acetate or polyester resin. The emulsion is made up of silver halide granules (silver bromide) in a gelatin matrix. This emulsion is sensitive to ionising radiation, visible and ultraviolet light. Double emulsion film has two emulsion one on each side of the base. See figure 1.2 for a diagram of film structure.

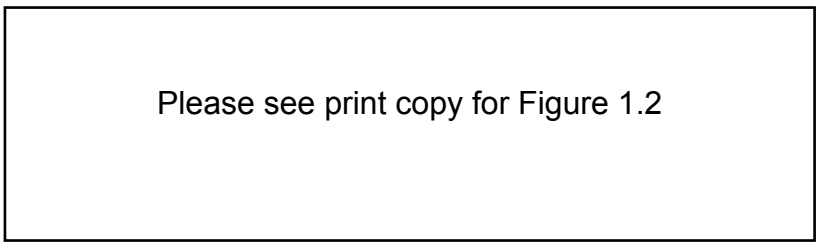

Figure 1.2 Cross section of an x-ray film. The base is cellulose acetate or a polyester resin, and the emulsion is usually silver bromide suspended in a gelatin matrix. (Reproduced from Medical Imaging Physics by Hendee and Ritenour 2002)

1.4.1.3.2 Photographic process

Incident radiation releases electrons in the medium (Hendee et al 2002). When these electrons hit the photographic emulsion they become trapped at sensitive centres in the silver bromide. Silver ions (Ag+) are neutralised by these electrons on the emulsion. The deposition of this metallic silver on the emulsion is a record of the information transmitted to the film by the incident radiation. The collection of all this metallic silver on the emulsion constitutes what is called the latent image.

After exposure the film is developed.

During the process of developing additional silver is deposited on the emulsion where the sliver ions were initially neutralised by the electrons. The latent image acts as a catalyst for deposition of metallic silver. No silver is deposited on the areas where there is no latent image. When the film is fixed the silver bromide granules which are not part of the latent image are removed by the sodium thiosulfate or ammonium thiosulfate present in the fixing solution. The amount of darkening on a film depends on the silver deposited in that region and consequently on the amount of radiation absorbed in that region.

Films may be calibrated using exposure to known doses of radiation. A densitometer is used to measure the optical density on the film which in turn is proportional to the absorbed dose.

The optical density is defined as OD = log (Io/I)

where Io- light measured without the film, I – light measure through an area on the film.

The readings are then corrected for base fog. Base fog is the OD measured in an unexposed film from the same batch and processed with the same film processor and same chemicals. Different film strips are exposed to different amounts of dose. From these measurements a Optical Density versus Dose curve can be produced. This system is the used to analyse films which have been exposed to radiation.

Film Dosimeters – Advantages and Disadvantages

Film has advantages when used in dosimetry including:

- high spatial resolution
- permanent record of exposure especially when used for routine Quality Assurance, for example in measurements of light vs radiation field congruence
- excellent imaging tool for patient set up during radiotherapy treatments

Film does have some disadvantage including:

- requires repeated calibrations for each film batch

- relies on reproducibility of chemical concentrations and developing cycle including temperature dependence

- relies on densitometry system

- the overall process is long and requires extreme care for reproducibility

1.4.1.4 Luminescent Detectors

Thermoluminescence dosimeters, or TLDs as they are usually known, are inorganic crystals which are generally non-conducting (Knoll 1989, Metcalfe et al 1997). The amount of literature on TLDs is vast and it is in itself a major field of research. The brief description here is a summary from some of the sources such as Knoll, Metcalfe et al and Kron.

The crystal structure has imperfections that act as energy traps between the valence and conduction band gap (Metcalfe et al 1997). When TLDs are exposed to radiation electrons are elevated from the valence band to the conduction band but during this process electrons are captured at energy traps (Knoll 1989). See figure below for schematic drawing showing this process.

If the energy level between the energy trap and the valence band is sufficiently large then there is a small probability that the electrons will fall back to the valence band (Knoll 1989). As the number of electron-hole pairs trapped in different energy levels increases it in turn is a measure of the amount of radiation deposited in the crystal (Knoll 1989). The method to liberate the electron-hole pairs from the energy traps is to apply thermal energy

or heat to the crystal structure and this action will cause the electrons and to fall to the valence band and then to the appropriate valence energy level. When this process takes place energy is released in the form of light. This light in turn is usually collected using a photomultiplier tube.

The amount of light released is dependent on the radiation absorbed by the TLD material. There are some commercial TLD readers that have automated system to reproduce this heating and readout process such as Rialto and Harshaw.

TLDs – Advantages and Disadvantages

TLDs have advantages when used in dosimetry including:

- availability in many different sizes and shapes which makes them suitable for QA dosimetry in many geometrical setups
- suitability for in vivo dosimetry for verification of patients treatment set ups and dose delivery.
- relatively inexpensive cost which facilitates their access in the clinical environment

TLDs do have some disadvantage including:

- a long TLD readout process which includes annealing cycles prior to readout and post readout, some post readout annealing processes may last up to 4 hours
- TLD materials do have energy dependence in the low energy regime, below 300keV
- Some TLD materials show sensitivity decrease known as fading where the signal output is reduced after a period of time
- TLDs need to be calibrated on a periodical basis

1.4.1.5 Semiconductor Detectors

Semiconductors have been widely used in Nuclear Spectroscopy and High Energy Physics due to their high energy, spatial and time resolution (Knoll 1989). Semiconductor dosimetry is an area which has been extensively researched. In general terms the principle of operation of a semiconductor detector is as follows: When an ionizing particle penetrates the p-n junction of the detector it produces electron-hole pairs along its track. An external electric field is applied between an anode and a cathode. The application of this electric field achieves charge collection when the electrons drift toward the anode and the holes drift to the cathode. The charge collected produces a current pulse signal which is then analysed with specialised electronic equipment.

1.4.1.5.1 Silicon Diodes

The key region of semiconductors based on silicon is the p-n junction. A p-n junction is formed at the junction of a p-type and an n-type semiconductor. A p-type semiconductor is produced when silicon is doped with impurities of electron acceptors (Knoll 1989, Metcalfe 1997). An n-type semiconductor is produced when silicon is doped with electron donors (Knoll 1989, Metcalfe 1997). When charged particles pass through the junction electron-hole pairs are formed to produce a current (Attix 1986). The junction can be biased or un-biased. When no bias is applied to the junction the direct current (DC) leakage current decreases faster than the current produced by radiation (Attix 1986). Therefore DC mode of operation is preferred in some areas of radiation detection.

1.4.1.5.2 MOSFETS

MOSFET stands for Metal Oxide Semiconductor Field Effect Transistor. Mosfets are relatively new detectors. They have been reported in the literature since the last 20 years (Thomson et al 1984, Butson et al 1996, Rosenfeld et al 1995).

When ionizing radiation hits the MOSFET the threshold voltage is changed. This change in voltage is proportional to the absorbed radiation. The voltage is read across the SiO_2 between the substrate and gate. A bias voltage si also applied however this can vary depending on the type and brand.

Semiconductors – Advantages and Disadvantages for Silicon Diodes and MOSFETS

Semiconductor-based dosimeters have advantages when used in dosimetry including:

- suitability for in vivo dosimetry for verification of patients treatment set ups and dose delivery.
- relatively inexpensive cost which facilitates their access in the clinical environment

Semiconductor-based dosimeters do have some disadvantage including:

- a temperature dependence is exhibited and this may become an issue when these devices are placed in contact with patient during in vivo dosimetry
- energy dependence is exhibited when they are used for dosimetry in beams where the quality is non-uniform
- angular dependence is shown when the incident radiation angle changes significantly, it is required to make many measurements to establish the conditions where this effect can be neglected

- when the they are exposed to high amounts of radiation permanent damage can occur, some semiconductors actually have a radiation beyond which they can no longer be used to detect dose reliably

1.4.1.5.3 Diamond Detectors

Diamond detectors are based on semiconductor technology and they have been reported in literature since 1980 (Heydarian et al 1993). Published work has investigated its fundamental properties as well as its radiation properties under radiation beams (Heydarian et al 1993, Hoban et al 1994). When ionising radiation is absorbed by the diamond electron-hole pairs are produced which produce electrical conductivity (W U Laub et al 1999). Natural diamond crystals are not suitable for dosimetry because they display a decrease in charge-collection efficiency (W U Laub et al 1999). But when they have the correct amount of impurities then they become suitable for radiation measurements. According to W U Laub et el (W U Laub et al 1999) the appropriate nitrogen concentration is of the order of less than 10^{-19} cm^{-3}.

Advantages of Diamond Detectors

Some of the advantages of diamond detectors include:

- good tissue equivalence for therapeutic photon and electron beams, 4-25 MV and 4-20 MeV respectively
- small size and therefore a good spatial resolution similar to diodes
- high sensitivity
- high resistance to radiation damage

1.5 Plastic Scintillators and Optical Fibres

Section 1.4 discussed a range of detectors that are currently used in radiotherapy dosimetry. The detectors included were: cylindrical ionisation chambers, parallel plate chambers, film, diodes, MOSFET and diamonds. The discussion included their advantages and disadvantages. A dosimetric system was developed with the purpose to measure photon beams produced by a linear accelerator.

The system consisted of 3 key elements. They were

- A plastics scintillator
- Optical fibre and
- Photodiode

In the context of the previous section the following presents a brief discussion on the advantages and disadvantages of plastic scintillators, optical fibres and photodiodes.

Advantages of plastic scintillators

These are the advantages of plastic scintillators

- water equivalence over the megavoltage energy range, this is very important for dosimetry in radiotherapy

- water equivalence above 100 keV, which is important for Iridium-192 dosimetry in brachytherapy

- temperature and pressure independence which means that no corrections have to be made for these

- they can be manufactured in different sizes and shapes, these properties can be used for spatial measurements where high resolution is required, for example, in x-ray penumbra regions

Disadvantages of plastic scintillators

- mechanical difficulty in coupling to optical fibres

- low light collection efficiency due to cylindrical geometry and due to lack of accepted protocol for surface smoothing

- energy dependence below 100 keV which is a disadvantage for kilovoltage dosimetry

Advantages of Optical Fibres

Optical fibres offer these advantages

-capacity to carry information over long distances

-no need for high voltages involved as the information is carried through optical means

-relatively low cost which enables easy access in the commercial market

Disadvantages of Optical Fibres

- production of Cerenkov noise in megavoltage radiation

- mechanical difficulty in coupling to plastic scintillators

- lack of ruggedness as compared to conventional triaxial cables

Advantages of photodiodes

Photodiodes as well offer the following advantages

-availability for use in optical devices which facilitated their use with optical fibres

-high sensitivity for production of visible light into electrical signal

-facilitation of optical light into charge or electrical signal for electrical processing to enable quantification of light production in plastic scintillator

Disadvantages of photodiodes

- temperature dependence

- mechanical difficulty in coupling to optical fibres

The following chapter will discuss plastic scintillators and optical fibres in more detail starting with a theoretical background, their application in radiotherapy, a discussion on the ideal system and finishing with the most current work in plastic scintillation dosimetry in radiotherapy.

Plastic Scintillators and Optical Fibres in Radiotherapy

2.1 Introduction

This chapter outlines the physical characteristics of plastic scintillator and their application in radiotherapy. A brief theoretical outline on organic scintillators is presented. The Cerenkov effect, which is a major source of noise in optical fibre when exposed to radiotherapy beams, is briefly described. A short review on the principles of refraction and total internal reflection in optical fibres is presented. This is followed by a review of the published results in the literature on the subject of developing a plastic scintillator system. The systems presented in this review include only the developments prior to the experiments performed for this project and presented in this thesis. This is followed by a section on what would be desirable in the ideal plastic scintillator system and the conditions required for this idealism. There have been further developments worldwide on this subject after the results presented in this thesis and they are summarised at the end of this chapter.

2.2 The Characteristics of scintillators and fibres

2.2.1 Classification of Scintillator materials

Scintillation materials can be classified as either organic or inorganic (Knoll 1989). Both type of materials are used for radiation detection depending on the application. Inorganic scintillators have the best output whereas the organic scintillators have a faster time response but their light out put is lower (Knoll 1989). In practical terms, organic scintillators are the preferred choice for beta spectroscopy and neutron detection

whereas inorganic scintillators are preferred for gamma-ray spectroscopy (Knoll 1989). Due to their physical composition organic and inorganic scintillators undergo different physical processes when they are exposed to radiation. The work presented in this thesis was mainly concerned with organic scintillators and their application in radiotherapy. The following paragraphs explain the physical processes involved in organic scintillators.

2.2.2 Physical process in organic scintillators

The molecular structure of a lot of organic scintillators is based on the π-electron structure. The π-electron energy levels are show in figure 2.1 below.

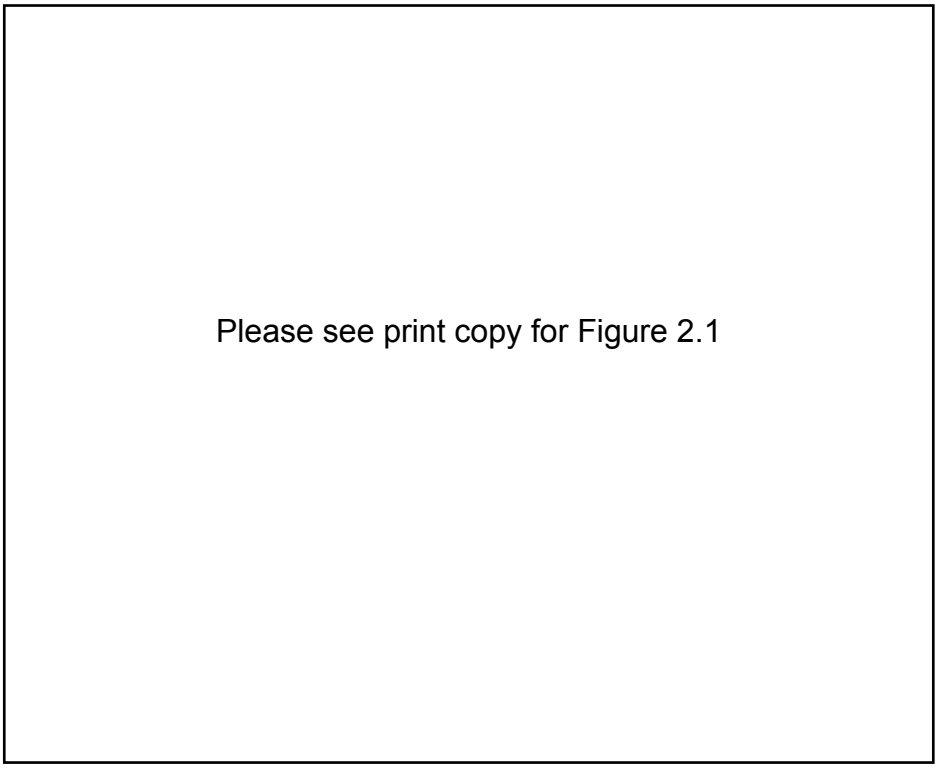

Figure 2.1 Energy levels of a π-electron structure. Reproduced from *Radiation Detection and Measurement* by F.G. Knoll, 1989.

The figure shows the configuration of a excited states. The excited states are divided into single and triplet states. Single states with spin 0 are labelled as S_0, S_1, S_2, S_3….and

the triplet states with spin 1 are labelled as T_1, T_2, T_3,….The energy spacing between S_0 and S_1 is of the order of 3 or 4 eV. The singlet states are subdivided into finer energy spacings. These finer energy levels correspond to vibrational states of the molecule, they are labelled as S_{00}, S_{01}, S_{02}, S_{03} and S_{10}, S_{11}, S_{12}, S_{13}.

When the plastic scintillator is exposed to ionising radiation, the kinetic energy carried by the charged particles passing through the medium is absorbed by the molecule. The figure represents this event by arrows pointing upwards. The higher singlet states S_2 and S_3 undergo radiation less internal conversion and as a result the S_{10} energy state becomes populated. The population of the S_{10} state is a very fast process lasting in the order of picoseconds.

Fluorescence is emitted when the energy level S_{10} is deexcited into the vibrational states of the ground energy level, S_{03}, S_{02}, S_{01} and S_{00}. The figure shows this process by arrows pointing downwards from S_{10} state to the sublevels of the ground state.
Phosphorecence occurs when the T_1 energy state deexcite into the ground energy state sublevels. This process is much slower than fluorescence.

The decay of fluorescence can be described mathematically by the following expression (Spieler 1998)

$$I(t) = I_o e^{-t/\tau f} - I_o e^{-t/\tau r}$$

Where Io = intensity at time 0

I(t) = intensity at time t

t = time

τ_f = fall time

τ_r = rise time

A representative plot of this mathematical function is displayed in figure below:

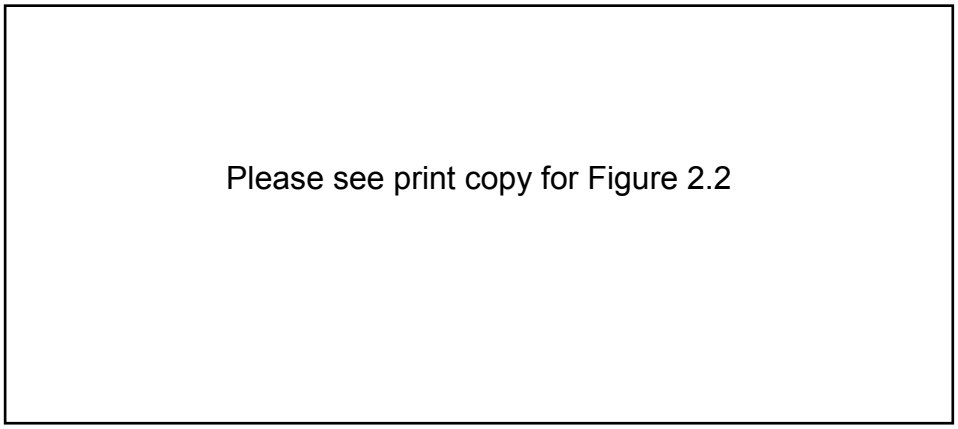

Figure 2.2 Fluorescence decay as function of time. Reproduced from *Introduction to Radiation Detectors and Eelectronics* by Helmuth Spieler, 1998.

2.2.3 Cerenkov Radiation

When the speed of a charged particle v, in a given medium exceeds the speed of light c/n in that medium, where n is the refractive index and c is the speed of light in a vacuum, then Cerenkov radiation is emitted (Knoll 1989). In contrast to scintillation light, Cerenkov light is produced along the direction of the charged particle velocity (Knoll 1989). Cerenkov emission occurs only when $n\beta > 1$, where β is the ratio of the charged particle velocity to the speed of light in a vacuum (Beddar et al 2006).The light is contained within a cone with vertex angle θ, where $\theta = \cos^{-1}(1 / n\beta)$.

2.2.4 Refraction and Total Internal Reflection in Optical Fibres

When a light ray in medium 1 is incident at angle θi at an interface a light ray is transmitted at angle θt in medium 2. This is called Snell's Law of Refraction. All angles

are measured relative to the normal perpendicular to the interface. The relationship between the refracted angle θt and the incident angle θi is n1sin θi=n2sin θt where n1 is refractive index for medium 1 and n2 is the refractive index for medium 2.

As θi is rotated through 90° θt will also rotate. The angle θi at which θt reaches 90° is called the critical angle θc. The critical angle θc is calculated by $\theta c = \sin^{-1}(n2/n1)$. This phenomena is shown in figure 2.3 below.

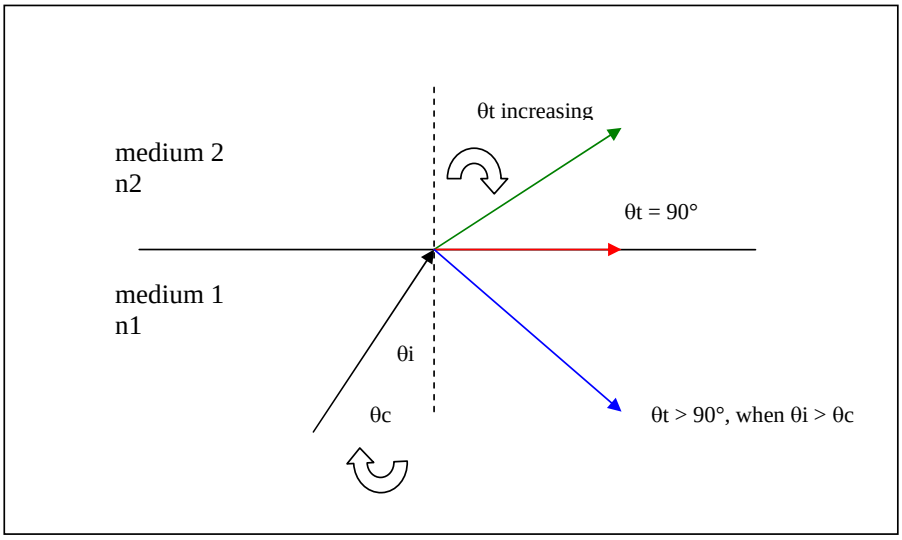

Figure 2.3 Principle of Refraction and Total Internal Reflection at boundary between medium 1 and medium 2.

When the incident angle θi is greater than θc the incident light rays are totally reflected back to medium 1. This is the principle of Total Internal Reflection and it is the effect by which light is guide inside optical fibres. Figure 2.4 shows the propagation of light rays inside an optical fibre. Incident light rays, red arrows, are first transmitted into the fibre core with refractive index n1 The transmitted light rays then hit the fibre clad with refractive index n2, where n1 > n2. These light rays are mostly reflected back into the core where they continue to undergo total internal reflection until the end of the fibre where they are again transmitted into the external medium.

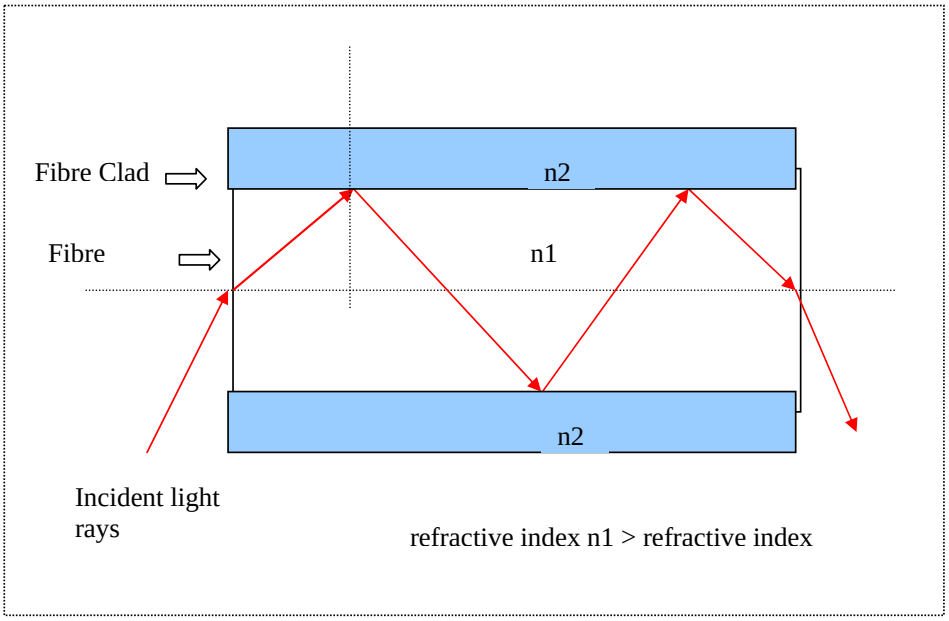

Figure 2.4 Total Internal Reflection in an Optical Fibre.

2.3 Applications in Radiotherapy

A relatively new family of detectors based on plastic scintillators has been developed over the last 15 years. Their progress has been limited due to various reasons which include technological and physical hurdles. What follows is a brief descriptive summary of the progressive development of plastic scintillator dosimetry applied in radiotherapy.

2.3.1 The Beddar System

In 1992 S. Beddar et al (Beddar et al 1992) reported a dosimetric system for Radiotherapy which used plastic scintillators as its key component. The system consisted of two identical optical fibres, each connected to a photomultiplier tube. One of the optical fibres was connected to a plastic scintillator but not to the second optical fibre. The signal from the second fibre measured the Cerenkov signal and was

Comment [A1]: Should you describe what that is?

subtracted from the signal of the fibre which had the plastic scintillator attached to it. All measurements published by Beddar et al were performed using this dual fibre system.

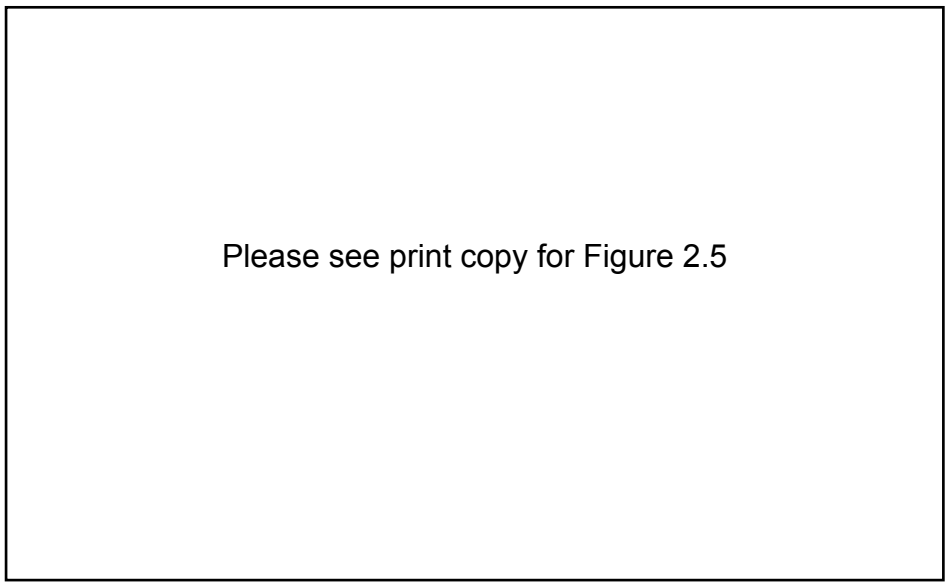

Figure 2.5 Plastic scintillator system as published by S. Beddar in 1992.

Beddar et al then proceeded to discuss the water-equivalence of plastic scintillators for high energy photon and high energy electron beams. The application of Burlin cavity theory showed that the energy dependence of plastic scintillators was equal or better than that of current systems, such as LiF thermoluminescent dosimeters, film and diodes. It was also shown that there was little temperature dependence and the radiation damage was much less than that exhibited by electron or photon diodes. Some of the other most important properties of plastic scintillators were their high spatial resolution, reproducibility, stability and linear response as a function of dose rate.

Comment [A2]: Would 'useful' be better?

2.3.2 The Meger Wells System

In 1994 C.M. Meger Wells et al (Wells et al 1994) published results which measured electron dose distribution near inhomogeneities. A plastic scintillator system similar to the one that Beddar et al developed and published was used. It was a dual fibre system with the second fibre running along side the fibre that had the plastic scintillator attached to it. The second fibre measured the signal produced by the Cerenkov effect. Meger Well et al concluded that the plastic scintillator detector was suitable for measuring electron dose distribution in heterogeneous fields. The scintillator detector measurements were in agreement with Monte Carlo calculations near inhomogeneities.

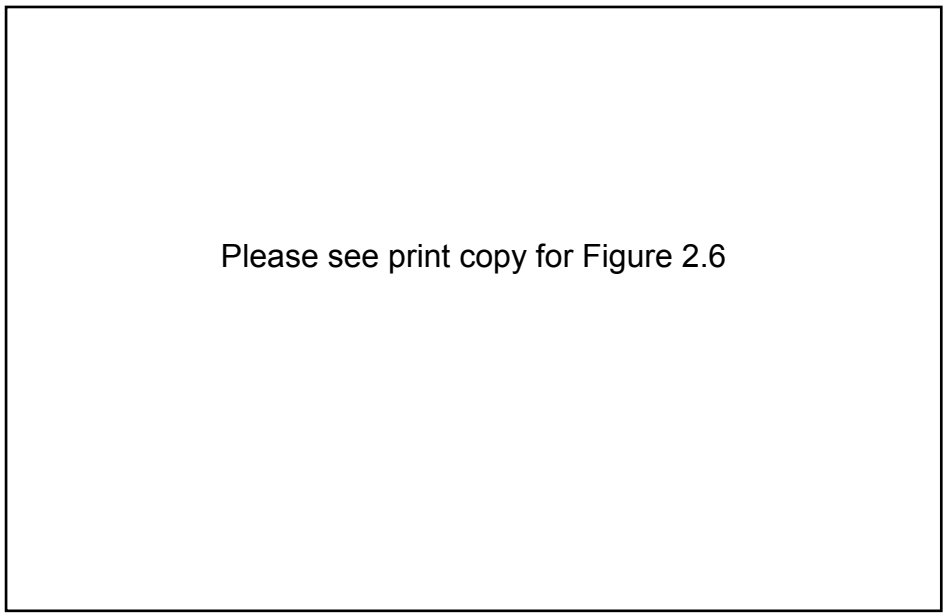

Figure 2.6 Plastic scintillator system as published by Meger-Wells in 1994.

2.3.3 The Aoyama System

In 1995 and 1996 T. Aoyama et al (Aoyama et al 1995, 1996) presented a scintillator-optical fibre detector which was also used for various radiotherapy measurements. The system was also a dual fibre detector similar to the detector presented by S. Beddar et al

and C.M. Meger Wells et al. However, there was one important difference with T. Aoyama's system. The very important difference was the electronic device used for collecting the light from the distal end of the fibres. Aoyama et al used a photodiode instead of a photomultiplier. This change made the system more compact, less expensive to manufacture and it added more practicality to the whole system. T. Aoyama et al published results obtained using an array of 12 fibres to measure an instantaneous depth dose profile for electron beams.

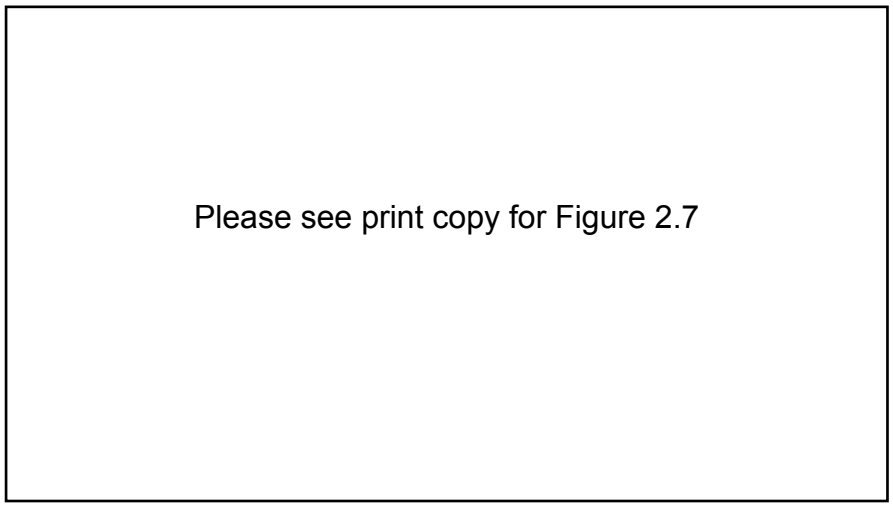

Figure 2.7 Plastic scintillator system published by T. Aoyama in 1995 and 1996.

2.3.4 The Letourneau System

In 1999 D. Letourneau et al (Letourneau et al 1999) published a paper on a scintillating detector which was similar to the detector published by S. Beddar et al in terms of being a dual optical fibre system except that the photomultipliers were replaced by photodiodes like T. Aoyama et al had previously published in 1995. D. Letourneau et al discussed their results and concluded that the spatial resolution of the scintillating detector was comparable to the resolution of a film-densitometer system.

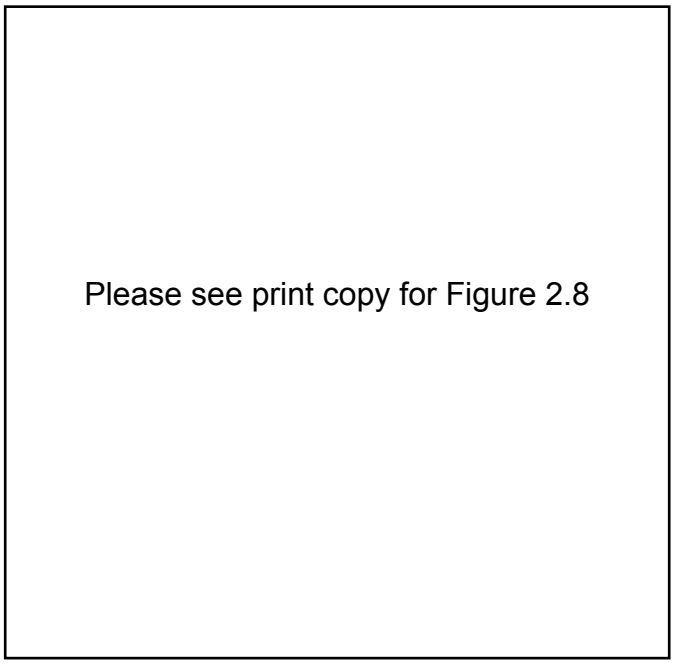

Figure 2.8 Plastic scintillator system published by D. Letourneau in 1999.

2.4 Optimal design for fibre system for dosimetry with linacs

2.4.1 Single channel vs dual channel

All systems described in section 2.3 operate on two channels to compensate for Cerenkov noise. However, these systems work on the assumption that the Cerenkov noise generated in each optical fibre is identical and in theory this allows the substraction and elimination of the Cerenkov noise. While this could prove to be true it could be argued that a better system would be one where there would be no need for a second channel to avoid any assumption in the electronic signal which is attributed to the dose measured by the plastic scintillator.

2.4.2 Choice of scintillator

The choice of scintillator was a crucial step in the design. A number of issues were taken into consideration in the selection of a suitable scintillator. Organic plastic

scintillators are water equivalent (Beddar et al 1992) and therefore possess the desired radiation properties for radiation detection in megavoltage x-ray beams.

2.4.3 Matching to fibre

In order to obtain a high degree of light collection, the choice of plastic scintillator was justified for the reason that plastic scintillators could be polished to maximise the transmission of light from plastic scintillator to optical fibre. This was a crucial step in the project since at the time of performing the experiments there was no standardised method to quantise the degree of polishing required to achieve 100 % transmission from plastic scintillator to optical fibre.

2.4.4 Match to detector

Light collection efficiency from the fibre to the electronic detector was a crucial stage. The choice of photomultiplier tube or diode was important for a number of reasons.

- Electronic Power Supply

Photomultiplier tubes usually operate on high voltage. Therefore they require a high voltage in the order of 1000V. This is not simple to obtain and one usually almost needs to buy high cost voltage components which undermines the simple aim to achieve a low cost and easy to assemble system. An additional factor is that using a two channel system would also double the high voltage electronic requirement.

- Wavelength matching

One key feature in the design is the correct matching of optical wavelength from optical fibre to electronic component. Both photomultiplier tubes and photodiodes show a response dependence as a function of light wavelength. Judgement had to be exercised as to the choice of photomultiplier tube versus diode. While photomultiplier tubes have

an internal amplification their high cost and high degree of difficulty in assembling the appropriate electronics was outweighed by the relatively ease and low cost of the diodes.

- Mechanical assembly from fibre to electronic component

Another key step during the design had to do with the most suitable mechanical mounting of the fibre onto either photomultiplier tubes or diodes. Low cost photomultiplier tubes did not have, at the time of performing the experiments, a proper adaptor to mount the fibre on to the photomultiplier tube. On the other hand, the diodes that were selected were specially design for use with optical fibre technology. Their design included the inclusion of a lens system which helped to focus the light signal from the fibre to the diode active area. The fibre was extremely easy to insert in the diode and the diode had a knob to tighten the coupling joint for stable and rugged use.

The ideal system would therefore need to have the following properties

- 100% light capture by the plastic scintillator
- 100% transmission at the plastic scintillator to the optical fibre interface.
- 0 % light loss along the conducting medium, optical fibre in this case. This means 0 % loss in internal reflection.
- 100% transmission at the optical fibre photodiode interface.
- 100% conversion from light to electronic signal by the photodiode.

Figure 2.9 below is a schematic representation of this ideal system.

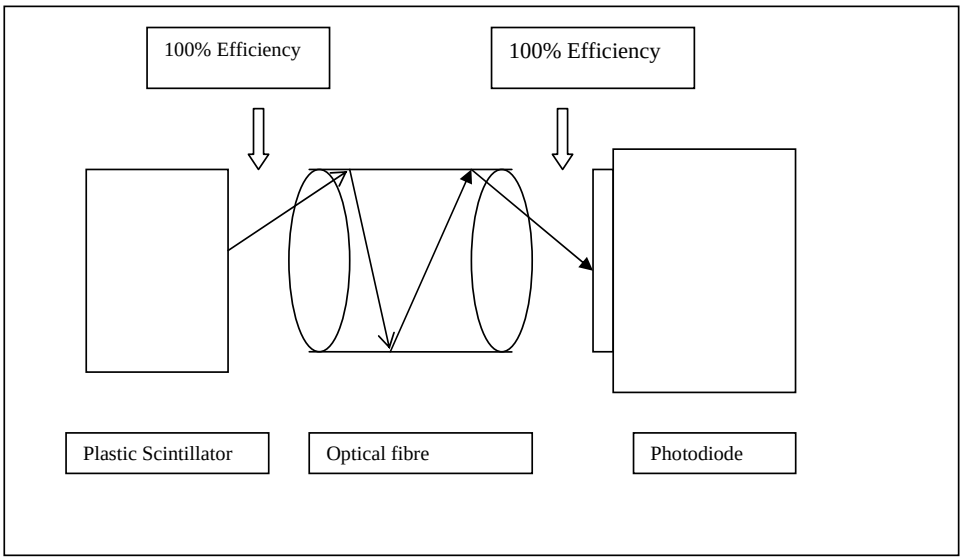

Figure 2.9 Schematic drawing of an optimal design. In an optimal design 100% of light produced by plastic scintillator would be transmitted to photodiode.

2.5 Subsequent developments in plastic scintillation dosimetry

Subsequent developments in plastic scintillation dosimetry include that of Clift et al (Clift et al 2000, 2002), Beddar et al (S. Beddar et al 2001, 2003, 2004, 2006), Archambault et al (L. Archambault et al 2005) and S. Law (S.Law et al 2006).

Clift et al (Clift et al 2000) published papers on the absorption filtration needed to reduce the noise due to Cereknov radiation. He published a paper that outlined his probe made up of long wavelength emitting scintillator, BC-430 coupled to a polystyrene light guide. He managed to lift the scintillator signal by a factor of 2.4 relative to the Cerenkov signal. He used a filter combination consisting of OG-530 and BG-40 Schott coloured glass. However, he concluded that optical filtration would be unlikely to reduce the Cerenkov noise in electron beams. In 2002, Clift et al (Clift et al 2002) published a paper on a method to temporary removal of the Cerenkov signal. This method worked efficiently in pulsed beams but it produced a reduction in light output as stated by Beddar (Beddar 2006).

Archambault et al (Archambault et al 2005) published on the comparison between different commercial models of scintillating fibres and plastic scintillators (BCF-12, BCF-60, SCSF-78, SCSF-3HF and BC-400, BC-408). He found that the intensity of the collected signal from the BCF60 with respect to the BC-400 was 47%. One of his main findings was symmetric detectors with almost the same resolution in both directions, 2 mm diameter by 3 mm length, could be made to produce signal of similar intensity to those obtained in asymmetric detectors.

Law et al (Law et al 2006) published a paper on the theoretical expression for the intensity of Cerenkov radiation transmitted in tunnelling modes within a fibre. One of the main findings by Law et al was that the angular distribution is independent of core/cladding refractive index and is independent of core size. However, the intensity of the Cerenkov radiation was proportional to the cube of the core radius. This finding implied that by selecting fibres with small core radius then noise from Cerenkov signal would be reduced.

Further to his papers of 1992, Beddar et al (Beddar et al 2001) published an article on a miniature scintillator-fiberoptic-PMT detector system for dosimetry of stereotactic radiosurgery fields. He also published an article on the efficiency of light collection by his plastic scintillator detector model (Beddar et al 2003). He produced mathematical calculations, based on current dosimetry models, which gave an indication of the magnitude of the total collection efficiency. This work was very important because it provided an insight into how efficient his system was. His main finding was that the main loss in transmission light by the whole system was the coupling of the plastic

scintillator to the optical fibre. He attributed this to two things: 1. the acceptance angle of the fibre and 2. the bonding material used for the plastic scintillator to optical fibre coupling. Furthermore, in 2006 Beddat (Beddar 2006) published an article which summarised the dosimetric characteristics and properties of plastics scintillators. He highlighted the fact that plastics scintillators don't require the usual conversion and corrections used for common detectors to convert readings into absorbed dose.

In context to the findings by Beddar (Beddar et al 2003) regarding coupling techniques the following chapter presents the coupling techniques that were used in this project. At the time of coupling optical fibres to photodiodes for this thesis, in 2001, there was very limited literature on this procedure.

Chapter 3

Coupling Techniques: Optical Fibre to Photodiode, Plastic Scintillator to Optical Fibre

3.1 Introduction

Chapters 1 and 2 have introduced the concept of constructing and assembling a radiation detector which has used plastic scintillators, optical fibres, photodiodes and photomultipliers tubes as its key components. What has been a critical step in the procedure to construct these detectors is the coupling technique employed in joining the different components. For detectors that are available in the commercial market this is not usually a concern because the products are already joined, assembled and ready to test. But for the research teams it has been a major step of the process.

This chapter presents the process and the outcomes obtained when the detector was being designed and assembled. At the beginning of the project it was decided to replicate as far as possible the design of the team led by S. Beddar (Beddar et al 1992). This meant using silica fibres. However, a photodiode was used, instead of a photomultiplier tube, as the key electronic component to convert the light signal into an electrical signal. This first design will be referred to as Design 1.

When using Design 1, it was found that the joint coupling the optical fibre to the photodiode was weak, brittle and it was not possible to strengthen it. A second method was therefore used which employed commercial components available in the optoelectronics industry. This second design will be referred to as Design 2.

This chapter presents the method used to join the optical fibre to the plastic scintillator. Only one method was used because it was found to be sufficiently strong and reliable for the experiments performed.

3.2 Design 1

Design 1 followed most suggestions given in the model published by S. Beddar (Beddar et al 1992) with the modification of changing the photomultiplier with a photodiode. The first step was to design a method to join the optical fibre to the photodiode. The following optical fibre, photodiode and transparent glue were used.

3.2.1 Silica Optical Fibre

Polymicro (Ohio, USA) silica fibre was used. This type of fibre, with part number FVP600660710, had a core of 600 ± 10 μm, a clad of 660 ± 10 μm and a buffer of 714 ± 10 μm. It had a High –OH silica core with doped silica clad and a polyimide standard buffer. It was a step index fibre with a numerical aperture of 0.22 and a full acceptance cone of 25.4 degrees. Its light transmission range was from 180nm to 1150nm.

3.2.2 Photodiode

A Perkins-Elmer silicon photodiode was used. This diode, with part number FFD-040B, was a large area, high speed N-type PIN Si photodiode. Its spectral response was in the range of 400nm to 1100nm. It had a photosensitive diameter of 1 mm and a fast response of 2 ns

3.2.3 Epotek Epoxy

A special glue was used to join the photodiode to the silica fibre. This glue was EPO-TEK UVO-114. This epoxy had a UV light curing cycle of 60 seconds for 340 mW/cm^2 at 365 nm. Its spectral transmission was specified as greater than 97% at a wavelength range of 500 – 1400 nm. Its refractive index was 1.519 at a wavelength of 589 nm.

3.2.4 Ultra Violet light source

Ultra Violet curing was achieved with a EFOS Ultracure 100SS system. This ultraviolet (UV) source was capable of light outputs of up to 20 thousand milliwatts per square centimetre for wavelengths between 250 and 500 nm. The ultraviolet light was transmitted through a liquid filled flexible light guide.

3.2.5 Joint Additional Strengthening

In addition to epoxy, a Teflon cap was made to strengthen the joint between silica fibre and the photodiode. This cap, as shown in figure 3.1, had a hole drilled in the middle of it through which the silica fibre was inserted. This hole had the dimensions of outer diameter of the optical fibre, which was approximately 1 mm.

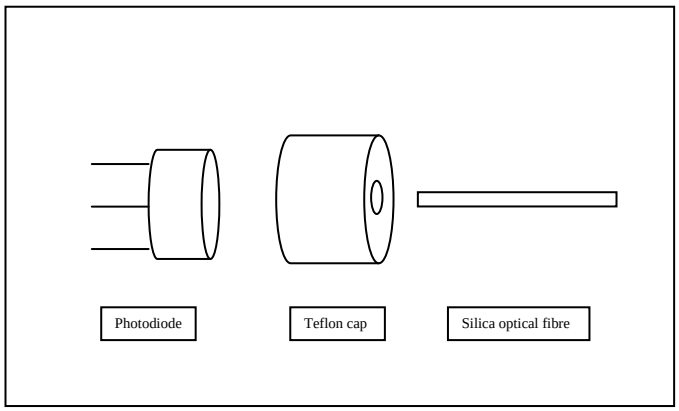

Figure 3.1 Schematic drawing representing the assembly of coupling photodiode to silica fibre.

3.2.6 Surface Polishing

The surface of this silica optical fibre was polished before being attached to the photodiode. Polishing involved two stages.

Stage 1:

- splice optical fibre
- place 600 grit abrasive paper on bench
- hold fibre and place on abrasive paper and slide it
- ensure sliding movement follows the shape of an eight number to achieve uniform polishing
- perform this coarse polishing until surface is smooth and no rough grooves are seen on the surface

Stage 2:

- using a 3 mm lapping film, slide the fibre in the same fashion as Stage 1. Make sure movement follows the shape of an eight number.
- continue polishing until a smooth surface is achieved.
- it is important to ensure that the surface is not angled with respect to the fibre axis as this could affect the collection of light from the plastic scintillator or the transmission of light on the photodiode

Please note that both ends of the fibre were polished, the end that connected to the plastic scintillator and the end which connected to the photodiode.

3.2.7 Coupling of Photodiode to Silica Optical Fibre

In order to couple the silica optical fibre to the photodiode a “pigtailing” jig provided by the University of Sydney was used. This jig was located at the Optical Fibre centre at

Redfern, Sydney. Below is a picture followed by a description of each of the components.

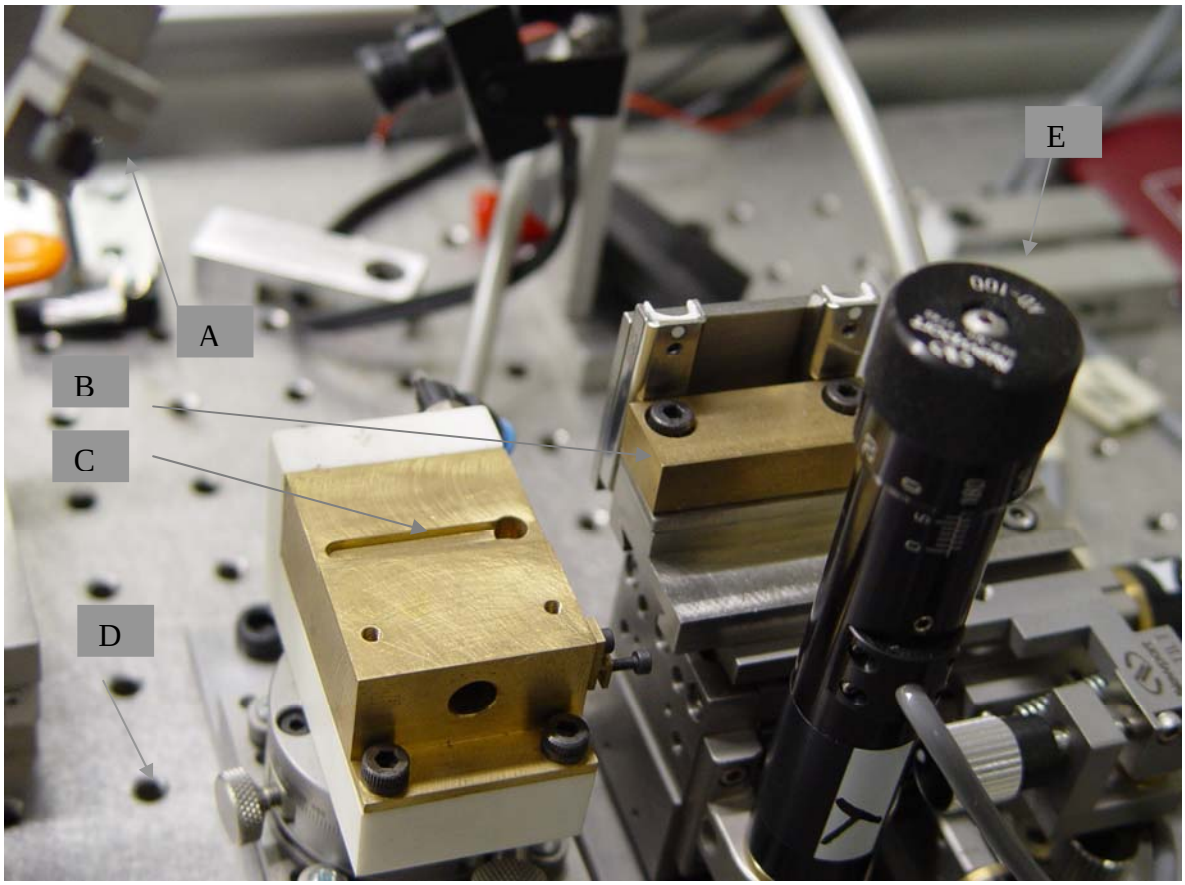

Figure 3.2 Customised assembling jig. Jig was used for coupling optical fibre to photodiode.

The jig was made up of the following parts:

Part A – Syringe holder. A syringe was filled with the respective epoxy material. The holder allowed free movement of the needle for pouring the epoxy drops where the fibre and diode were joined together.

Part B – A brass metal block was fabricated for the purpose of supporting the fibre. This block had a special air adaptor. The air adaptor allowed its connection to the air suction

mechanism. The air suction mechanism allowed the fibre to be held firmly on the metal for the duration of the UV curing or overnight curing.

Part C – This brass metal block was redundant in this set up but had a similar function to Part B. It was included so that the precise positional calibration of the jig could be used.

Part D – Vibration-proof bench. This bench was especially designed to absorb any floor or building vibration. This allowed the isolation of the whole system from any unforeseen vibrational changes due to structural building vibrations.

Part E – Vernier scaling system. Part B was mounted on this system which allowed Corse and Fine adjustment. Very precise positioning of the components was possible with this system using the x, y, z axis controls.
A microscope also formed part of the system. It is not shown in the picture. This microscope sat above the jig. Its purpose was to magnify an image of the joint. Viewing through this microscope allowed very fine adjustment of the joint.

3.2.8 Ultraviolet Curing

As mentioned before the ultraviolet curing involved shining a 340 mW/cm^2 ultraviolet beam on the joint for a length of 60 seconds. Two pictures showing this technique are displayed below. The first picture, figure 3.3, shows the optical fibre, epoxy and photodiode before UV curing. The second picture (figure 3.4) shows the same as the first picture but during UV light curing.

Figure 3.3 Silica Alignment of silica optical fibre on photodiode prior to ultraviolet curing. Epotek epoxy was poured between the silica optical fibre and the photodiode.

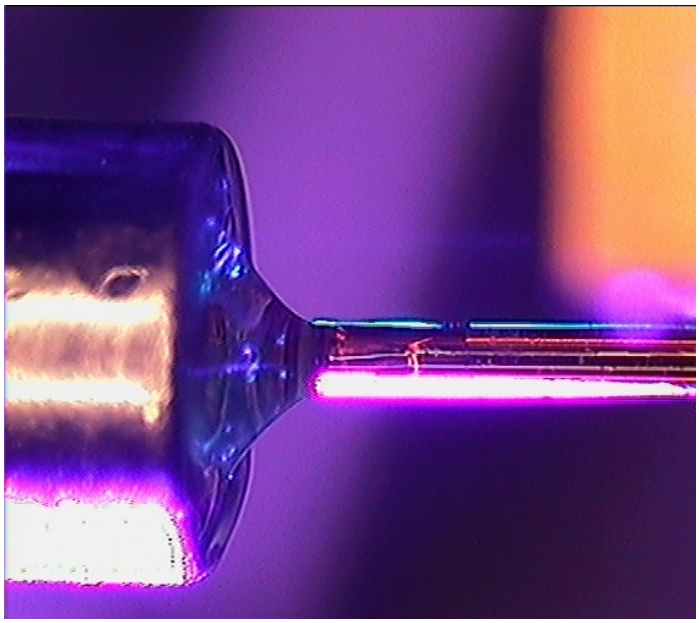

Figure 3.4 Ultra Violet curing. Purple colour shows ultraviolet beam on epotek epoxy.

After UV curing was performed it was necessary to wrap the fibre with a heat plastic shrinking material to protect it from the environment. The picture of the final outcome for the Design one is shown below in figure 3.5.

Figure 3.5 Picture of Design 1. Photodiode contacts were soldered on BNC triaxial connector.

Black shrink plastic was used to seal joint from environmental light.

Unfortunately, the use of silica optical fibres resulted in a brittle coupling to the photodiode that failed before completion of initial experiments.

3.3 Design 2

Since Design 1 broke during measurements it was concluded that a different design was needed in order to improve the model. A search was conducted in the commercial catalogues to find a photodiode that was stronger, more robust and that had been intended for frequent use. The search led to a photodiode and to optical fibre described in the following section.

3.3.1 Optical Fibre

This is an optical fibre which had been specifically designed for use with a specific photodiode, which is presented in section 3.3.3. The core material for this fibre was Polymetyl-Methacrylate Resin. It had a cladding material of Fluorinated Polymer, its core refractive index was 1.49. The profile for the refractive index was step index and a numerical aperture of 0.50. The core diameter was between 920-980 μm and the cladding diameter was between 940-1000 μm.

3.3.2 Photodiode SFH250

The photodiode was manufactured by Infineon Technologies. This SFH250 diode had a Photosensitivity spectral range λ of 400-1100 nm with a maximum at 850nm, as shown in figure 3.6, a capacitance of 11 pF, a photocurrent of 3 mA when reverse biased at 5V, a temperature coefficient of -0.04 %/K, a dark current of 1nA. This photodiode had a special advantage. It had a moulded microlens for focusing the light emitted from the fibre and focused on the photodiode. The photodiode housing had a special aperture for inserting and locking in optical fibres of 1 mm diameter.

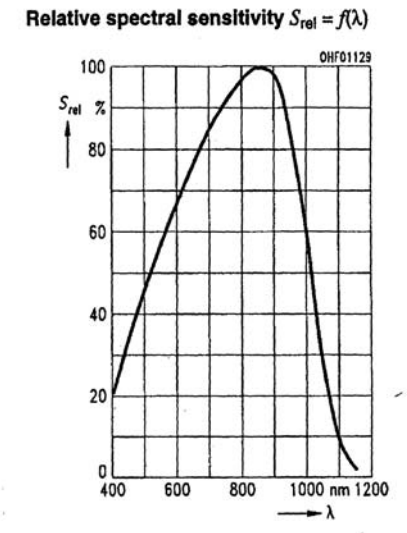

Figure 3.6 Spectral sensitivity of SFH250 photodiode

3.3.3 Plastic Scintillator

The scintillator used for Design 2 was BCF-60 (Bicron). Its emission was green colour with a peak at 530 nm and a decay time of 7 ns. Its core material was Polystyrene with core refractive index of 1.60, a density of 1.05 and a numerical aperture of 0.58. The cladding material was Acrylic with a refractive index of 1.49. This scintillator was classified as a scintillating fibre due to its structure. The advantage of this scintillating fibre was its increased ability to trap the light emitted by itself as the principle of internal reflection applied here. The machining of a pure scintillator to a small diameter was not so easy at all and for that reason the structure of this scintillating fibre was an advantage.

3.4 Attachment of Plastic Scintillator to Optical Fibre

The attachment of the optical fibre to the plastic scintillator involved the making of a Perspex cap. A cavity was drilled in the centre of a Perspex cylinder with a diameter of the same dimension as that of the optical fibre. The optical fibre used in Design 2 had a dimeter of approximately 1 mm. Figure 3.7 shows a diagram of the cylinder.

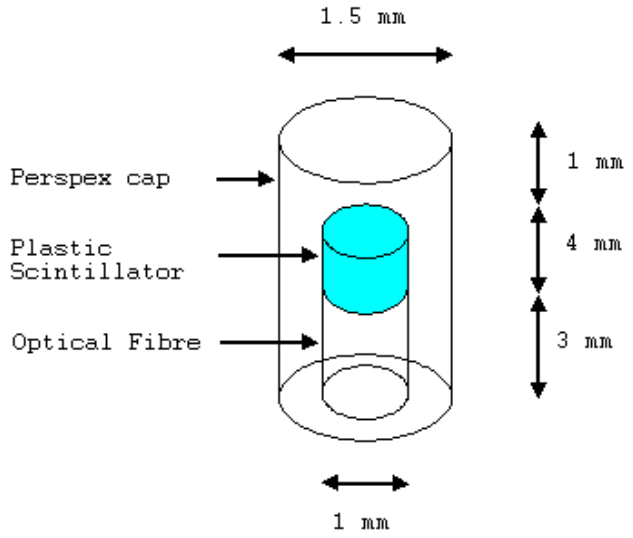

Figure 3.7 Attachment of Plastic Scintillator to Optical fibre.

The depth of the drilled cavity was approximately 7 mm. The length of the plastic scintillator inserted into this cavity was 4 mm. Consequently the length of the fibre that fitted into the cavity was approximately 3 mm. The advantage of using a cylinder as shown in figure 3.4 was its relative ease of manufacture and its remarkable strength. It must be pointed out at this stage that a robust detector was desirable for the purpose of reproducibility and stability in both mechanical and dosimetric terms. The coupling of optical fibres of such small diameters tended to be weak and fragile. The added strength over the scintillator to fibre joint was a crucial point and a key achievement in the development of this system.

3.5 Plastic Scintillator Polishing

The plastic scintillator was polished on both surfaces. After cutting the 4 mm scintillating fibre both ends were very rough. Polishing was performed in a similar fashion as described in section 3.2.6. It is important to emphasize that the polishing of both plastic scintillator and optical fibre was somewhat subjective as there was no proper quantifying method to determine an absolute measure of the polishing. This is a

major drawback as it provides no baseline for polishing any of the optical surfaces in these systems.

The following chapter will present the results obtained with Design 2. A discussion of the results obtained will also be presented and followed by a theoretical analysis of these results as well as a comparison with commercial detectors.

Chapter 4

Methodology and Experimental Work

4.1 Introduction

Previous publications have described how other researchers have measured radiotherapy beams with plastic scintillators at depth (chapter 3). The incident photon beam produces secondary electrons at depth in water which give rise to the Cerenkov effect. It is these electrons which became the subject of interest in order to measure the Cerenkov signal detected by the optical fibre. In order to obtain the right signal from the plastic scintillator it was necessary to measure the profile in two stages. One stage included the measurement of the Cerenkov signal only and stage two involved the measurement of both the Cerenkov signal and the plastic scintillator signal simultaneously. To obtain the right signal these two signals were subtracted from each other.

The measurements required the use of a motorized water tank (Wellhofer). This water tank was filled with water and placed under the gantry of a Siemens Primus linear accelerator.

Figure 4.1 Wellhöfer water tank place under Siemens linac.

The photon beam used was produced by a Siemens Primus linear accelerator which had the following specifications.

Table 4.1 Siemens Primus Linear Accelerator specifications for 10x10cm^2 at 100 cm Source to Surface Distance

Nominal Energy	Depth of dose maximum	Percentage Depth Dose at 10cm depth
6 MV	1.5 cm	67.7 %
10 MV	2.5 cm	74.5 %

In order to establish the performance of the developed system other commercial detectors were used to measure the beam profile so that a direct comparison against commercially available dosimeters could be performed.

4.2 Methods

4.2.1 Experimental set-up for beam profile measurement in Water using Optical fibre and Plastic scintillator

A Blue Phantom (IBA, Wellhöfer) water tank was used as the medium in which the beam profile was scanned. This water phantom is shown in figure 4.1. The energy of the photon beam was 6 MV produced by a Siemens linear accelerator. The Source to Surface Distance was set to 100 cm and the field size was 10x10 cm^2 at isocentre. Each exposure comprised of 100 Monitor Units.

The optical fibre was mounted on the ion chamber holder of the water tank scanning arm (see figure 4.2).

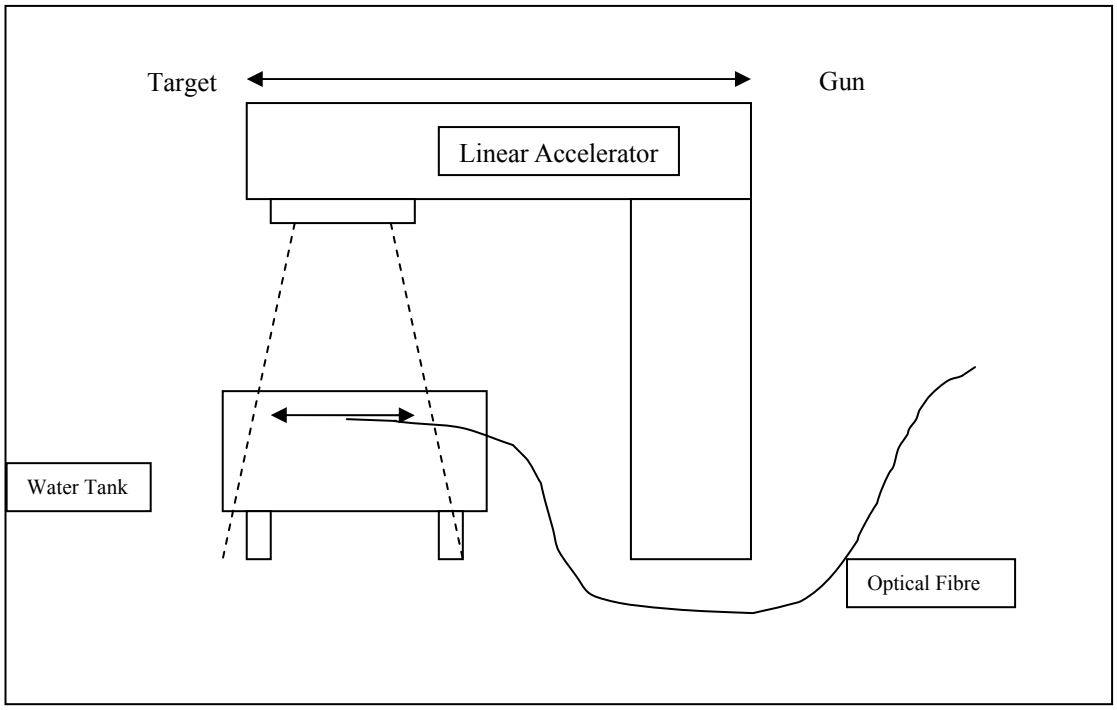

Figure 4.2 Drawing showing the direction of scanning for 6MV photon profile

The scanning motion was performed in the in-plane direction, i.e. the Gun to Target direction. Measurements were taken at discrete points along the gun target plane, and the position accuracy of this system was ±0.5 mm. This fine and small step motion was achieved using the OmniPro software which was designed specifically to drive the water tank system. The mode operation for scanning was manual. What this means is that the detector was driven one step a time to take each of the measurements.

The following profiles were measured with:

1: The fibre without any scintillator (Cerenkov)

2: Scintillator plus fibre (Luminescence + Cerenkov)

4.2.2 Experimental set-up for beam profile measurement in water using commercial detectors: CC04, CC13, PFD and SFD

In order to compare the performance and validity of the profile measured with the scintillator, the measurement was repeated under the identical conditions with 4 other commonly used detectors. These detectors were: CC04 (cylindrical compact chamber), CC13 (cylindrical compact chamber), PFD (silicon diode) and SFD (silicon diode).

Table 4.2 Commercial Detectors Specifications

Detector	Sensitive volume material	Sensitive volume dimensions	Effective scanning width, "resolution" Inner radius (ion chamber) Diameter (Diode)
CC04	Air	0.04 (cm^3)	2.0 mm
CC13	Air	0.13 (cm^3)	3.0 mm
PFD	Silicon	Diameter = 2mm Thickness = 0.06 mm	2.0 mm
SFD	Silicon	Diameter = 0.6 mm Thickness = 0.06 mm	0.6 mm

These 4 detectors were specifically designed for use with the Blue Phantom (IBA, Wellhöfer). These detectors were mounted on the water tank using their factory made holders. The scanning performed with these detectors was motorized by using a reference dosimeter in the field. This method of scanning is well known in radiotherapy and it is the accepted practice for measuring beam profiles with motorized water tank systems.

4.3 Results

4.3.1 Results obtained with Optical fibre and Plastic Scintillator

Figures 4.3 and 4.4 display the raw results obtained for the experimental set up explained in section 4.2.1. Figure 4.3 displays the results that were measured with the optical fibre only without the plastic scintillator attached to it. These readings are expressed as a percentage of the signal measured by the optical fibre when the plastic scintillator was attached to it.

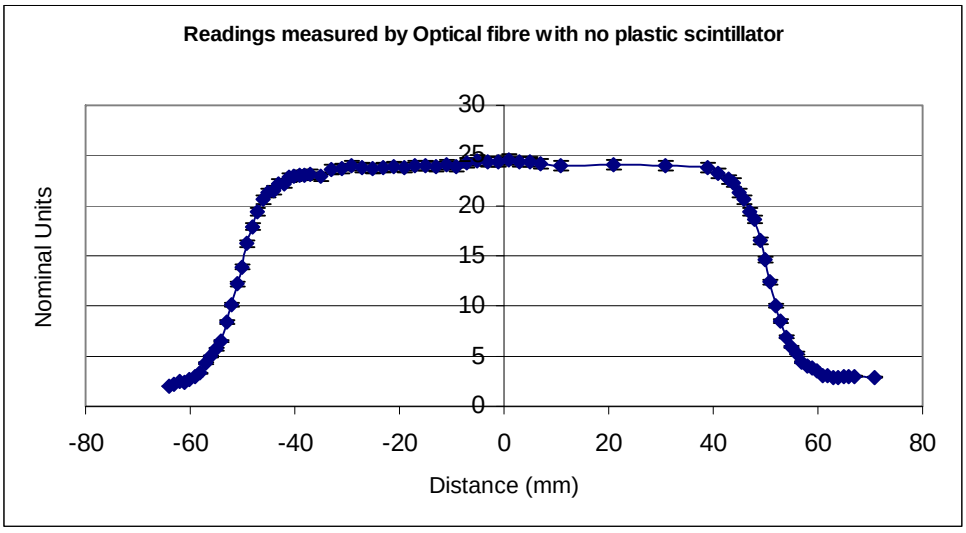

Figure 4.3 Readings measured by optical fibre with no plastic scintillator.

Figure 4.4 display the readings obtained by the plastic scintillator when it was attached to the optical fibre. OmniPro software was used to normalise these readings to the value on the central axis.

Figure 4.5 below shows the signal attributed to the plastic scintillator only. The signal was obtained by substracting the result of figure 4.3 from figure 4.4. Figure 4.5 was smoothed and normalized by OmniPro software.

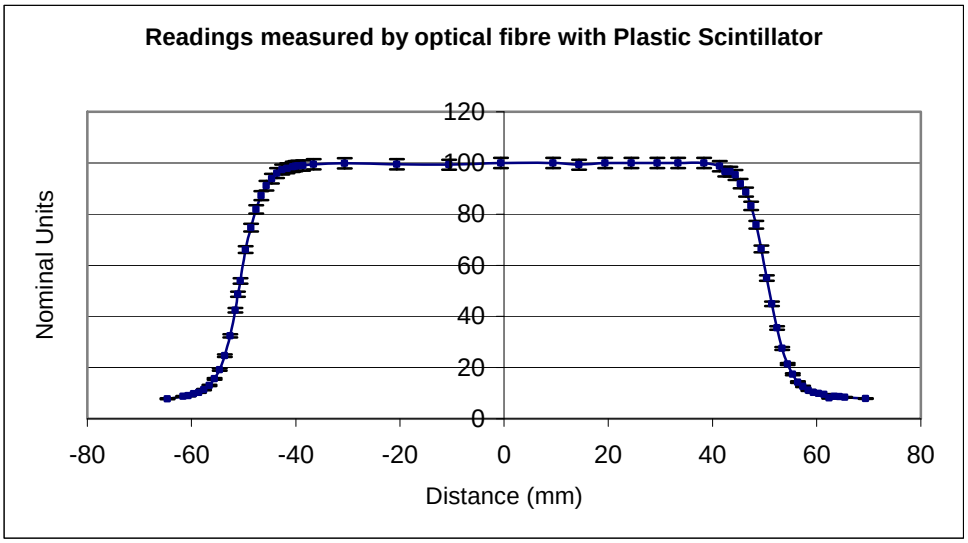

Figure 4.4 Readings measured by optical fibre when plastic scintillator BCF60 was attached to it.

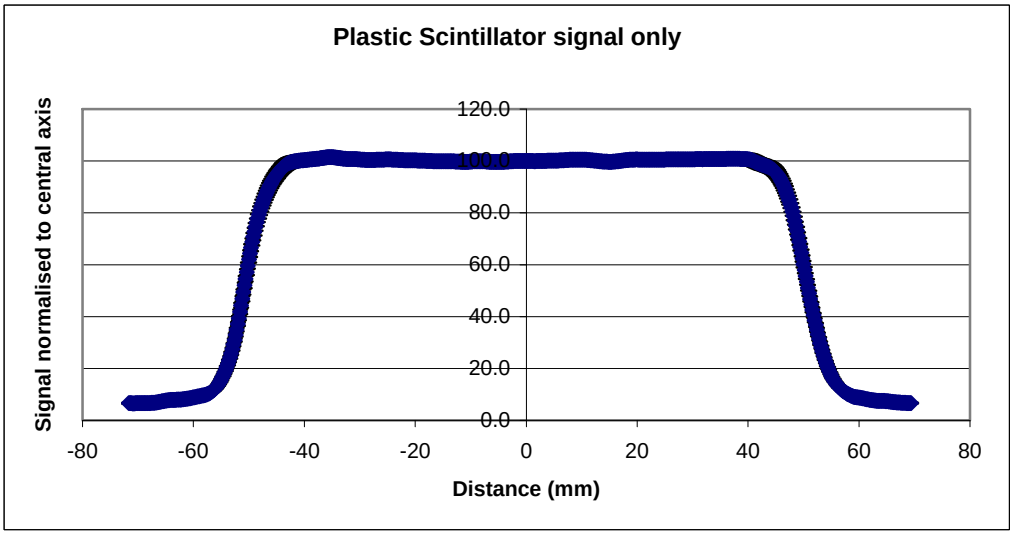

Figure 4.5 Plastic scintillator signal. Signal was extracted from readings from figures 4.3 and 4.4.

4.3.2 Results obtained with other detectors: CC04, CC13, PFD and SFD

The results obtained from the experiments explained in section 4.2.2 are shown in figures 4.6 to 4.9. All these figures were normalized to 100% at the central axis. Shown in figure 4.6 are the readings obtained by the compact chamber CC04.

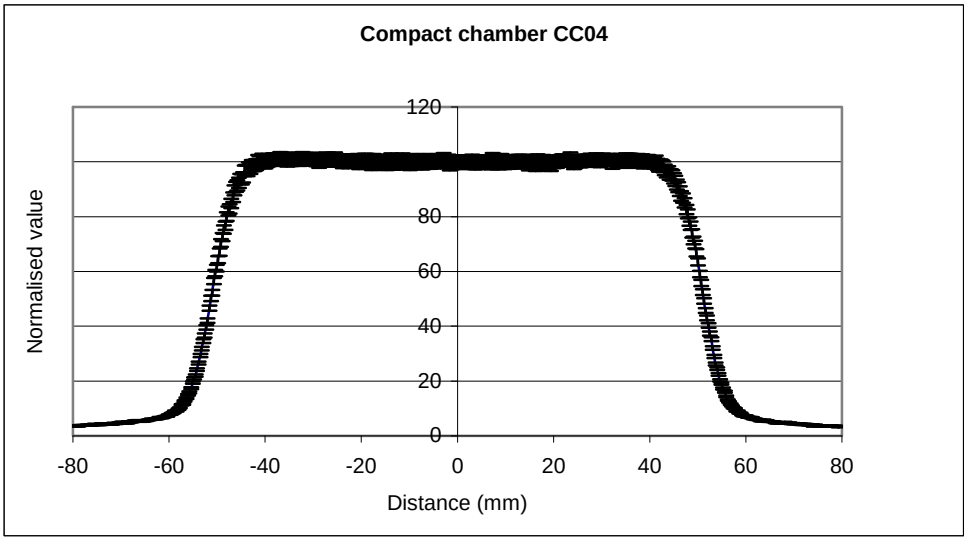

Figure 4.6 6MV photon beam profile measured by ion chamber CC04 at 1.5cm depth.

Figure 4.7 below shows the readings obtained with compact chamber CC13.

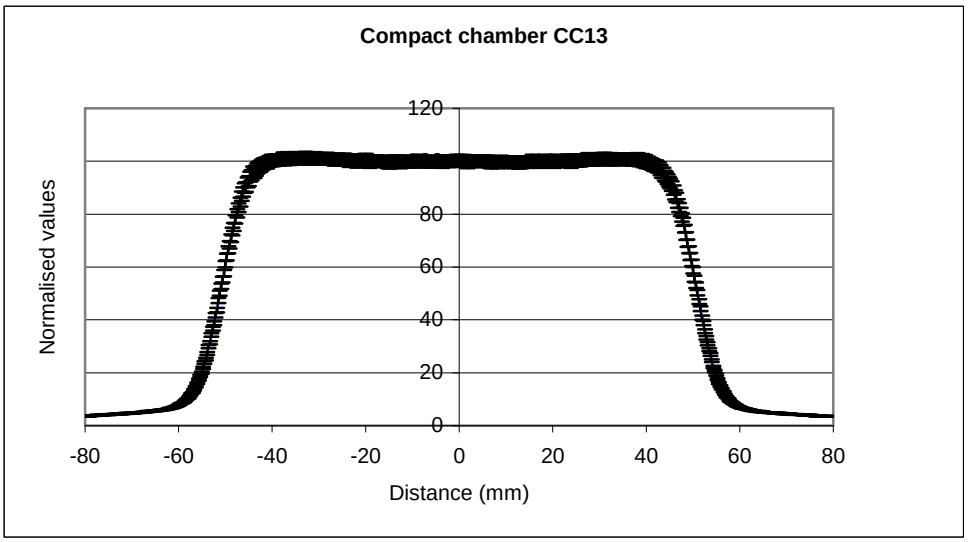

Figure 4.7 6MV photon beam profile measured by ion chamber CC13 at 1.5cm depth

Figure 4.8 below shows the results obtained with commercial diode PFD.

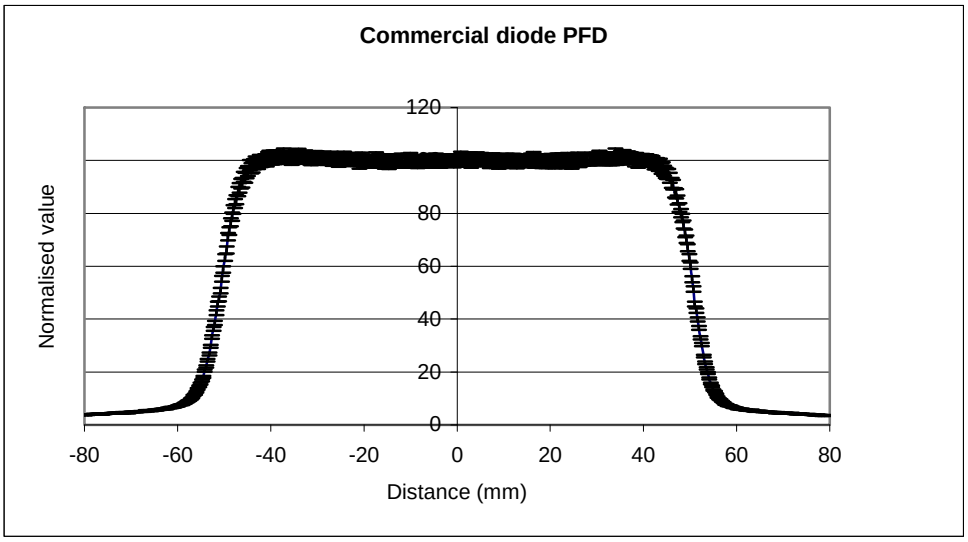

Figure 4.8 6MV photon beam profile measured by commercial diode PFD.

Figure 4.9 below shows the results measured with a commercial diode SFD.

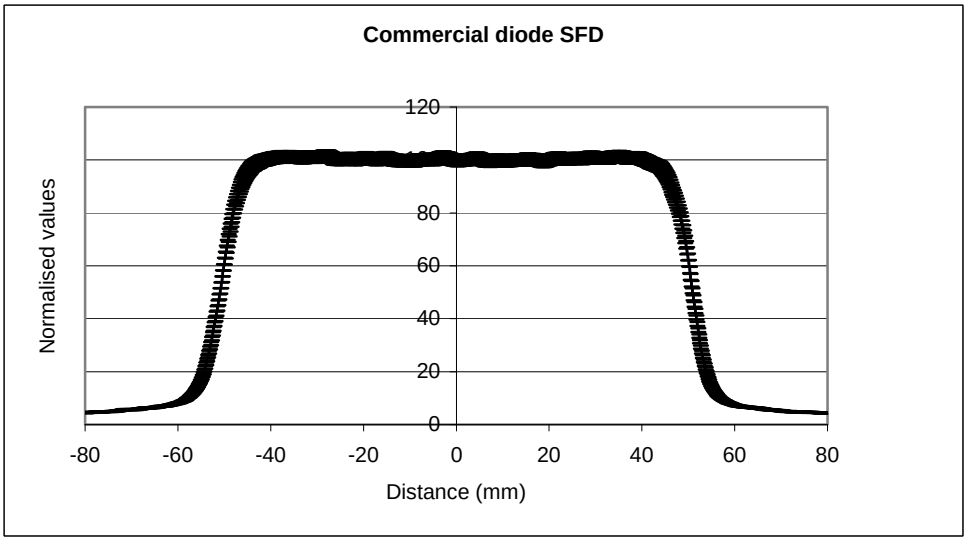

Figure 4.9 6MV photon beam profile measured by commercial stereotactic diode SFD at 1.5cm depth.

4.4 Discussion of Results

In order to analyse and to objectively present the results obtained with the plastic scintillator system, a comparison was carried out between the results measured with the plastic scintillator and the results obtained with the other detectors. This comparison was performed by

- The gamma evaluation method. This method consisted of a combination of dose difference and distance to agreement (DTA) analysis as outlined by Low et al (Low et al 1998).

4.4.1 Justification for the Gamma Evaluation Method

When medical physicists commission new equipment or treatment planning systems they need to compare a set of measured values against a standard reference set or a known set of values. One example is the commissioning of planning systems where calculated data by the planning system is compared against measured data. A qualitative evaluation of the calculated data is made by either superimposing the isodose distributions by hand or by using software. While this practice is fairly common it might be argued that it is rather subjective than objective depending on the degree of rigorousness employed by the medical physicist. In ideal terms, it is desirable to obtain a comparison which can be quantified and compared against acceptable criteria of proper tolerance values for the parameters used in the criteria. Such degree of sophistication has been achieved with the gamma evaluation method. This method was first proposed by D.A. Low et el. and it has been incorporated into planning systems such as Eclipse (Varian, Palo Alto, USA).

The relevance of this method with respect to the research presented here relates to the comparison between a standard or reference profile in water and the measured values by

the plastic scintillator. Strictly speaking, the gamma evaluation method is a quantified and objective method to assess how close is the profile measured by plastic scintillator to the reference profile. The reference profile in this instance was chosen to be the profile measured with the ion chamber CC13, in figure 4.7. The main reason behind this decision was because of the fact that this later profile was accepted as the baseline profile, for these conditions, by a clinical radiotherapy department.

4.4.2 Description of the Gamma Evaluation method

Daniel A. Low et al and W.B. Harms et al provide a very good and detailed description of the gamma evaluation method. A short and brief description is reproduced here for explaining and clarifying how the analysis was carried out for the present work in this thesis.

Figure 4.10 below shows a diagrammatic representation of the composite analysis by the mathematical formalism that describes the dose-difference and distance-to-agreement (DTA).

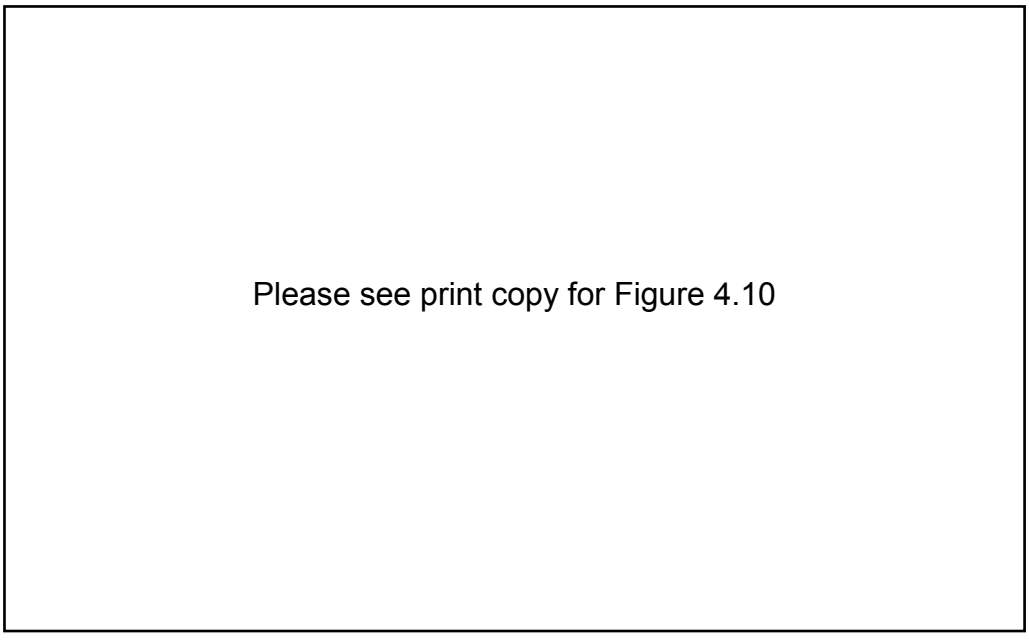

Figure 4.10 Gamma method in two dimension. Reproduced from Low et al.

Figure 4.10 a) shows a point, $\mathbf{r}_m$, which lies at the origin of the figure. The axes x and y represent the spatial location $\mathbf{r}_c$ of the calculated value relative to the point at the origin. The δ axis, which is perpendicular to x and y, represents the difference between the measured value $D_m(\mathbf{r}_m)$ at point $\mathbf{r}_m$ and the calculated value $D_c(\mathbf{r}_c)$ at point $\mathbf{r}_c$. The DTA criterion, Δd_M, is represented by a disk in the $\mathbf{r}_m - \mathbf{r}_c$ plane with a radius equal to Δd_M. The evaluation then states that if the calculated distribution surface $D_c(\mathbf{r}_c)$ intersects the disk, the distance-to-agreement DTA is within the acceptance criterion and the calculation passes the test at that particular point. The vertical line represents the dose-difference test, its length being $2\Delta d_M$. The evaluation also states that if the calculated distribution crosses the line (if $|D_c(\mathbf{r}_m) - D_m(\mathbf{r}_m)| \leq \Delta D_M$) then the calculated distribution passes the dose-difference test at that particular point.

An improved version of this method considers both dose-difference and DTA criterion simultaneously. This is achieved by selecting an ellipsoid as the surface representing the acceptance criterion. This situation is represented in figure 4.11 shown below.

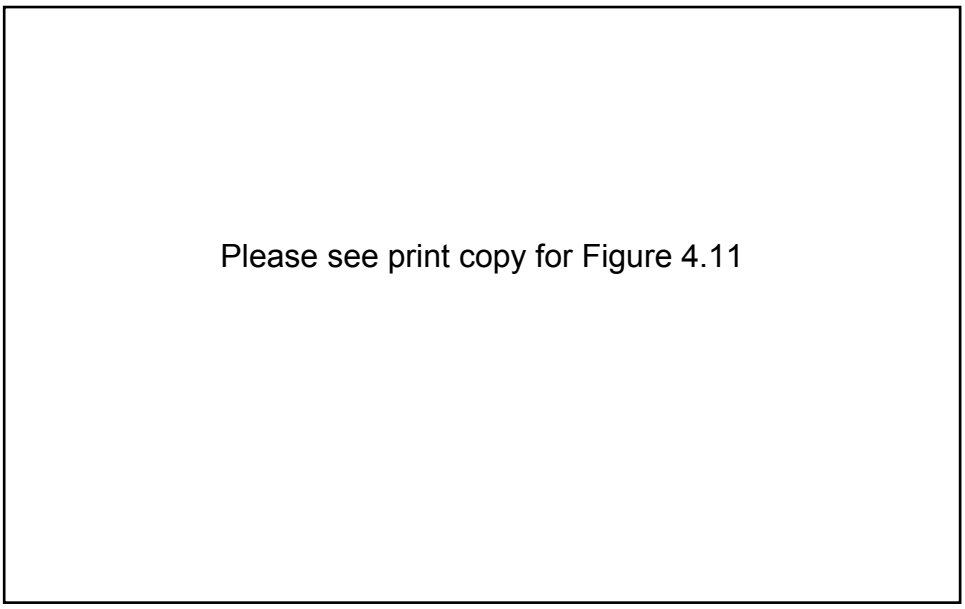

Figure 4.11 Gamma function reproduced from Low et al.

The equation that represents the ellipsoid surface is

$$1 = \sqrt{\frac{r^2(\mathbf{r}_m, \mathbf{r})}{\Delta d_M^2} + \frac{\delta^2(\mathbf{r}_m, \mathbf{r})}{\Delta D_M^2}},$$

Figure 4.12 Equation of an ellipsoid surface. Reproduced from Low et al.

where

$r(\mathbf{r}_m, \mathbf{r}) = | \mathbf{r} - \mathbf{r}_m |$ and $d(\mathbf{r}_m, \mathbf{r}) = D(\mathbf{r}) - D_m(\mathbf{r}_m)$ is the dose-difference at position $\mathbf{r}_m$.

The evaluation states that if any portion of $D_c(\mathbf{r}_c)$ surface intersects the ellipsoid than that calculation passes at position $\mathbf{r}_m$. This definition allows for a general comparison between calculation and measurement.

The quantity on the right hand side of equation is defined as the quality index $\Gamma(\mathbf{r}_m,\mathbf{r}_c)$ i.e.

$$\Gamma(\mathbf{r}_m,\mathbf{r}_c)=\sqrt{\frac{r^2(\mathbf{r}_m,\mathbf{r}_c)}{\Delta d_M^2}+\frac{\delta^2(\mathbf{r}_m,\mathbf{r}_c)}{\Delta D_M^2}},$$

Figure 4.13 Gamma function. Reproduced from Low et al.

where $r(\mathbf{r}_m,\mathbf{r}_c) = |\mathbf{r}_c - \mathbf{r}_m|$ and $\delta(\mathbf{r}_m, \mathbf{r}_c) = D_c(\mathbf{r}_c) - Dm(\mathbf{r}_m)$.

What is important to realize here is that the pass-fail criteria is:

$\gamma(\mathbf{r}_m) \leq 1$, calculation passes the test,

$\gamma(\mathbf{r}_m) > 1$, calculation fails.

4.4.3 Analysis of Plastic scintillator results using the Gamma Evaluation method

4.4.3.1 Plastic Scintillator versus CC13

For the purpose of analyzing the measured profile at depth as measured with the plastic scintillator system, the measurement obtained with the ion chamber CC13 was used as the reference one. The passing criterion used to for the analysis was $\Delta D_M = 3\%$ and $\Delta d_M = 3$ mm. These results were plotted and analysed in a spreadsheet and are graphically represented in figure 4.14 below. The figure shows the profiles measured by the ion chamber CC13, the plastic scintillator on the same scale where all values have been normalized to be one at the centre. The graph also shows a trend line at level 1.0 on the vertical axis. The purpose of this line is to show that region where the γ evaluation

function either passes or fails the criterion. The gamma function is also shown as it was calculated with the specified criteria $\Delta D_M = 3\%$ and $\Delta dM = 3$ mm.

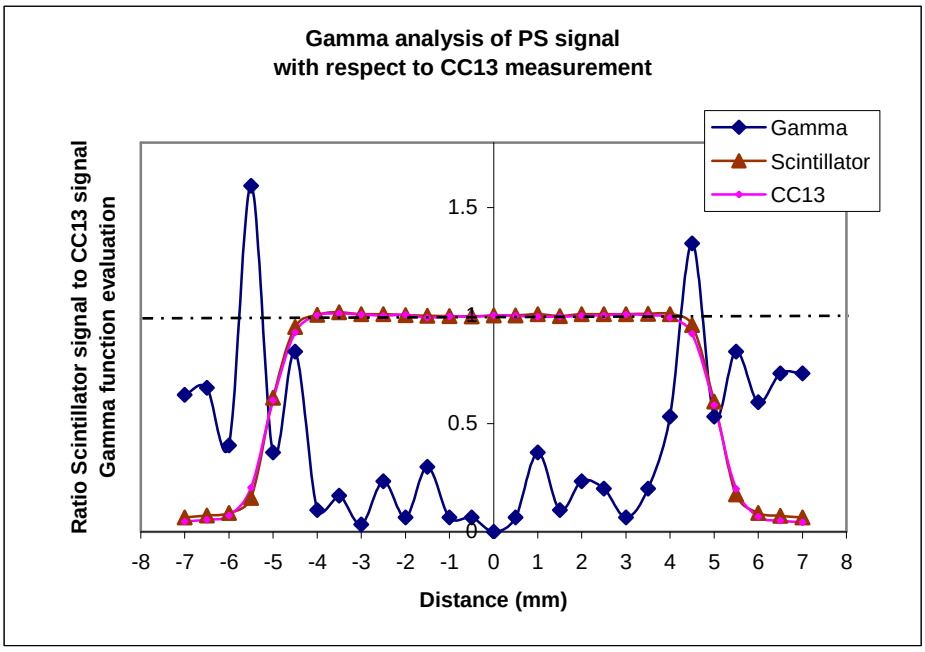

Figure 4.14 Gamma function evaluation for CC13 and Plastic Scintillator.

It is important to realize that while a qualitative visual inspection would lead to believe that both curves actually agree with each other the quantitative method suggests that there is a region of disagreement at -5 to -6 cm and 4 to 5 cm distance from the centre or from the vertical axis.

It must also be noticed that besides those two regions the rest of the measured area by the plastic scintillator agrees well with the measurement performed with ion chamber CC13.

Furthermore, the gamma value recorded and shown in figures 4.14 to 4.17 was maximum in figure 4.14, with an approximate value of 1.5. Whereas in figures 4.15 to 4.17 the maximum gamma value was approximately 1.4 or less. The possible reason for this was the superior spatial resolution of the plastic scintillator to the CC13 ion chamber. The spatial resolution of the plastic scintillator was closer to the commercial diodes and the ion chamber CC04 as shown by the lower gamma values. Laub (Laub et

el 2003) discussed the volume effect and detector size of in the dosimetry of steep dose gradients. According to their findings the plastic scintillator would be comparable to ion chamber 0.3 cm^3 chamber.

4.4.3.2 Plastic Scintillator versus CC04

The profile measured with the plastic scintillator was also compared with the profile measured by the small volume ion chamber CC04. The Gamma Evaluation function was used to compare the two profiles. The passing criterion used for the analysis was $\Delta D_M = 3\%$ and $\Delta d_M = 3$ mm. Figure 4.15 below displays these results.

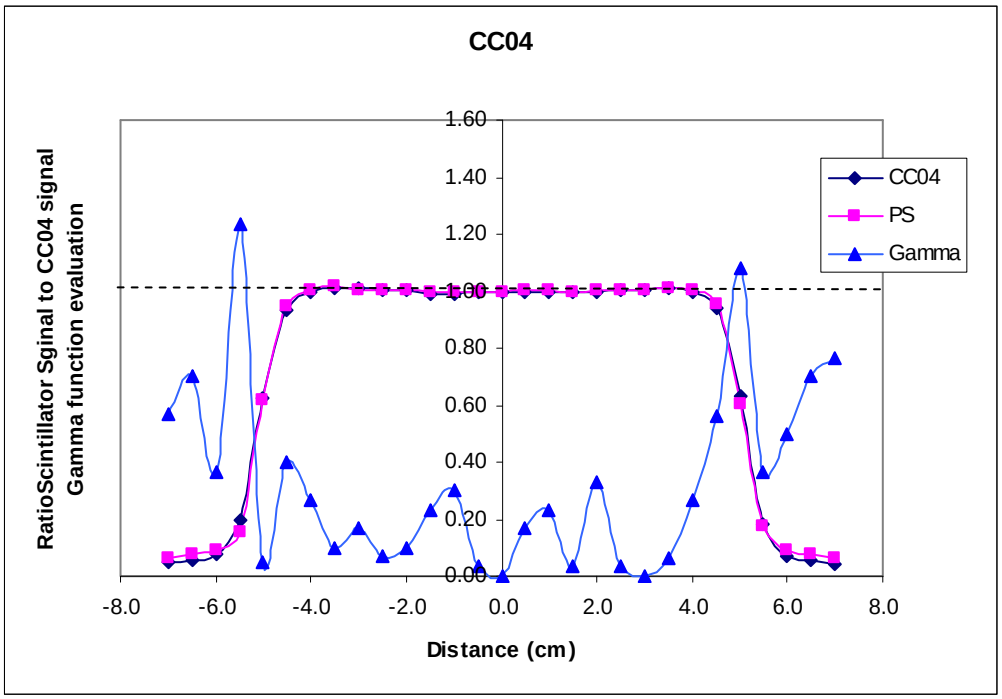

Figure 4.15 Gamma evaluation function for CC04 and Plastic Scintillator.

4.4.3.3 Plastic Scintillator versus PFD

The profile measured with the plastic scintillator was also compared with the profile measured by the commercial photodiode PFD. The Gamma Evaluation function was used to compare the two profiles. The passing criterion used for the analysis was ΔD_M = 3% and Δd_M = 3 mm. Figure 4.16 below displays these results. It is evident in this figure that there is an asymmetry in the gamma function. This could be attributed to a probe misalignment with respect to the central axis when the diode was mounted on the water tank. A correct alignment would have helped reduce the gamma value on the positive side and resulted on a lower gamma value.

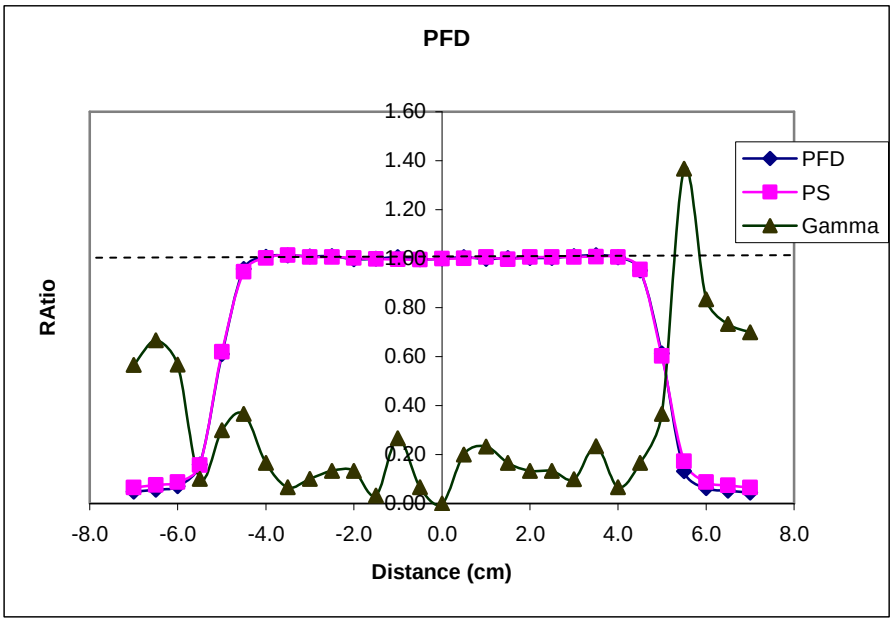

Figure 4.16 Gamma Evaluation function for PFD and plastic scintillator.

4.4.3.4 Plastic Scintillator versus SFD

The profile measured with the plastic scintillator was also compared with the profile measured by the commercial stereotactic photodiode SFD. The Gamma Evaluation function was used to compare the two profiles. The passing criterion used for the analysis was ΔD_M = 3% and Δd_M = 3 mm. Figure 4.17 below displays the results. An asymmetry can be observed in the gamma function and this could be attributed to a misalignment when the diode was mounted on the water tank. A correct gamma value could have

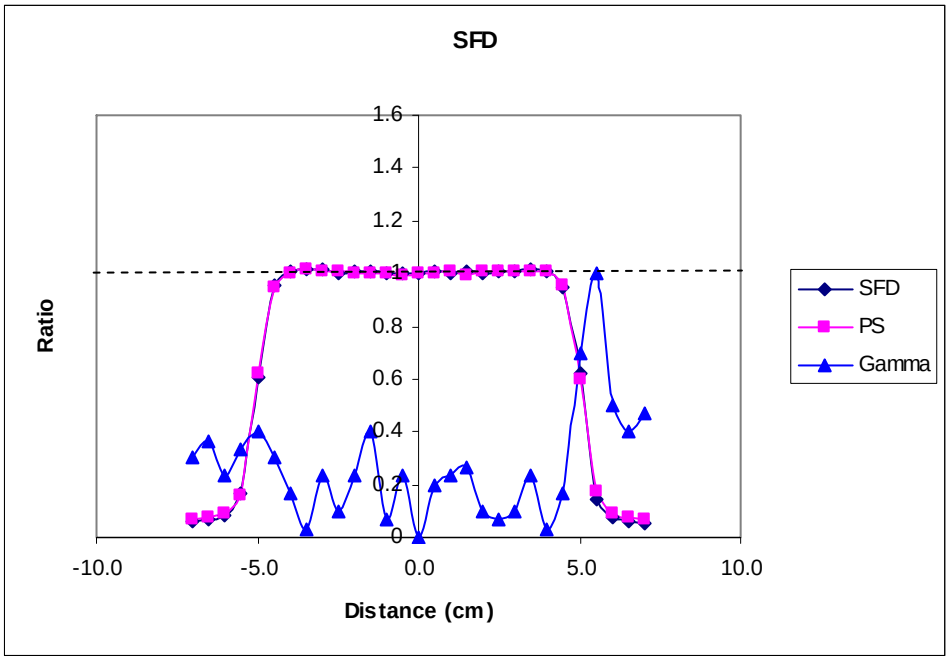

Figure 4.17 Gamma evaluation function for SFD and plastic scintillator.

Chapter 5

Conclusion

The conclusions that follow from work presented in this thesis are as follows:

5.1 Technique to couple optical fibre to photodiode for Design 1

In relation to the method to couple the optical fibre to the photodiode it was demonstrated that the joint formed by coupling a silica fibre to a photodiode proved to be weak, brittle and breakable. This joint only lasted for 6 months.

5.2 Coupling of optical fibre to photodiode for Design 2

Since the initial method for Design 1 failed, a commercial photodiode was tested and used for this project. This photodiode was specifically designed for use with optical fibre in the telecommunication industry. This particular photodiode had a focussing lens embedded in its housing to focus the light from the optical fibre on to the active surface area of the photodiode. It was concluded that this photodiode was the best choice for this system and it was subsequently used for the experiments performed in water phantom under a 6 MV x-ray beam.

5.3 Technique to couple plastic scintillator to optical fibre

Initial testing at OFTC demonstrated that it was very difficult to join objects which had a very narrow diameter, in the order of 125 – 1000 μm. Therefore a simple and robust method was designed to join a plastic scintillator to an optical fibre. The method

involved making a Perspex cap to encase the plastic scintillator on to an optical fibre. Epotek epoxy 301 was the glue used to join the two pieces together.

5.4 Substraction of Cerenkov signal

For the work presented in this project, the same optical fibre was used to measure a x-ray beam profile at depth in water. By using the same optical fibre the need to use more sophisticated electronic set up was eliminated. The systems described in chapter 2 did use a dual channel system and this required setting up more elaborate electronics to compensate and balance the signals produced in the optical fibres as a consequence of Cerenkov electrons.

Therefore it can be concluded that although the results obtained were good, the method presented in this thesis proved to be time consuming and in a real scenario it would prove to be impractical. The need to develop a system which uses only one optical fibre remains the greatest challenge in the development of plastic scintillation in radiotherapy.

5.6 Gamma evaluation analysis

The gamma evaluation was used to compare the results obtained by the plastic scintillator with results obtained with commercially available detectors. This method showed how to quantify the discrepancy between the reference value and the experimental value. The reference value was taken as the readings obtained with the ion chamber CC13. The results obtained with the plastic scintillator were compared with all the commercial detectors and it was found that the plastic scintillator detector passed the criterion of Dose Difference = 3% and Dose-To-Agreement = 2 mm.

5.7 Future Work on Plastic Scintillation dosimetry in radiotherapy

As stated at the beginning of this thesis the aim was to develop a plastic scintillator system that comprised the use of a single optical fibre. Numerous researchers (Beddar et al 1992, de Boer et al 1993, Wells et al 1994, Aoyama et al 1995, Le´tourneaua et al 1999, Clift et al 2000, Archambault et al 2006) have attempted many different methods to accomplish this objective and to date no single system has been implemented in the mainstream of the radiotherapy physics community as a commercially available detector system. The work presented in this thesis itself shows how difficult it is to construct and test a plastic scintillator system.

The characteristics of plastic scintillators are very desirable and therefore more work needs to be undertaken to achieve a reasonable compromise between Signal-to-Noise ratio and spatial resolution to produce a system that is greatly needed in the modern small field techniques currently used in radiotherapy such as stereotactic radiosurgery and Intensity Modulated Radiation Therapy.

Although the above mentioned researchers have almost exhausted methods to eradicate Cerenkov signal and noise still there is no published work on the next generation of optical fibres which are Hollow Optical waveguides. A Hollow Optical waveguide may include a core dielectric material equivalent to air. This would have the obvious implication of allowing the speed of light in air to be faster than the charged particles, electrons in this case, in the core medium. One would expect minimum production of Cerenkov light.

More work could also be carried out in the composition and production of light in plastic scintillators themselves. No study on Monte Carlo modelling of light production in the plastic scintillator with a focus on the megavoltage spectrum has been published. In 1999 Williamson et al published a paper on the development of new plastic scintillation materials for low energy photons in Brachytherapy. Their work included maximizing sensitivity and radiological equivalence to water by measuring the response, defined as ε (light output/unit air kerma), of plastic scintillators to low-energy photons emitted by $^{99m}T_C$, ^{192}Ir, and ^{137}Cs sources (Williamson et al 1999).

In a similar fashion a study on the composition of current plastic scintillator material could be carried out to increase the light output where Cerenkov emission is minimal.

Another area of research could be the improvement of electronic circuitry. For example, Clift et al published an article on the use of slow plastic scintillators to separate the scintillator signal from the Cerenkov signal using time properties. While the experimental result was promising, the method to separate the electronic signals involved the use of oscilloscopes. Work could be carried out on designing a single circuit board that could perform these tasks and thus provide an integrated system for signal processing.

Although the radiotherapy community seems to have reached a temporary dead end in the quest for a commercial plastic scintillator system there still exists the hope that major improvements in technology will allow us to fulfil the dream of developing a robust, practical and affordable plastic scintillator detector.

References

1. Aoyama T., Maekoshi H., Tsuzaka M. and Koyama S. 1995 A scintillating fiber beam-energy monitor for electron beam therapy. Med. Phys. 22, 2101–2102.

2. Attix F. H. 1986 Introduction to Radiological Physics and Radiation Dosimetry.

3. Archambault L., Arsenault J., Gingras L., Beddar A. S., R. Roy and L.Beaulieu 2005 Plastic scintillation dosimetry: Optimal selection of scintillating fibers and scintillators. Med. Phys. 32, 2271–2278.

4. Archambault L., Beddar A. S., Gingras L., Roy R. and L. Beaulieu 2006 Measurement accuracy and Cerenkov removal for high performance, high spatial resolution scintillation dosimetry. Med. Phys. 33, 128–135.

5. Beddar A. S., Mackie T.R. and Attix F.H. 1992 Water-equivalent plastic scintillation detectors for high-energy beam dosimetry: I. Physical characteristics and theoretical considerations. Phys. Med. Biol. 37 1883-1900.

6. Beddar A. S., Mackie T.R. and Attix F.H. 1992 Water-equivalent plastic sc intillation detectors for high-energy beam dosimetry: II. Properties and measurements. Phys. Med. Biol. 37 1901-1913.

7. Beddar A. S., Mackie T. R., and Attix F. H, 1992 Cerenkov light generated in optical fibres and other light pipes irradiated by electron beams. Phys. Med. Biol. 37, 925–935.

8. Beddar A. S. 1994 A new scintillator detector system for the quality assurance of 60Co and high-energy therapy machines. Phys. Med. Biol. 39, 253–263.

9. Beddar A. S., Kinsella T. J., Ikhlef A. and C. H. Sibata 2001 A miniature scintillator-fiberoptic-PMT detector system for the dosimetry of small field in stereotactic radiosurgery. IEEE Trans. Nucl. Sci. 48, 924–928.

10. Beddar A. S., Law S. H., Suchowerska N., and T. R. Mackie 2003 Plastic scintillation dosimetry: Optimization of light efficiency. Phys. Med. Biol. 48, 1141–1152.

11. Beddar A.S., Suchowerska N., Law S.H. 2004 Plastic scintillation dosimetry for radiation therapy: minimizing capture of Cerenkov radiation noise. Phys. Med. Biol. 49, 783-790.

12. Beddar A.S. 2006 Water equivalent plastic scintillation detectors in radiation therapy. Radiation Protection Dosimetry, Vol. 120, No 1-4, pp1-6.

13. Butson M., Rozenfeld A., Mathur J.N., Carolan M., Wong T.P.Y. Metcalfe P.E. 1996 New radiotherapy surface dose detector: The MOSFET. Med. Phys 23, 655-658.

14. Clift M.A., Sutton R.A., and Webb D.V., 2000 Dealing with Cerenkov radiation generated in organic scintillator dosimeter by bremsstrahlung beams. Phys. Med. Biol. 45, 1165-1182.

15. Clift M.A., Sutton R.A. and Webb D.V. 2000 Water equivalence of plastic organic scintillator in megavoltage radiotherapy bremsstrahlung beams. Phys. Med. Biol. 45, 1885-1895.

16. Clift M.A., Johnston P.N. and Webb D.V. 2002 A temporal method of avoiding the Cerenkov radiation generated in organic scintillator dosimeters by pulsed mega-voltage electron and photon beams. Phys. Med. Biol. 47, 1421-1433.

17. de Boer S. F., Beddar A. S. and J. A. Rawlinson 1993 Optical filtering and spectral measurement of radiation-induced light in plastic scintillator dosimetry. Phys. Med. Biol. 38, 945–958.

18. Epoxy Technology 2008 http://www.epotek.com/SSCDocs/datasheets/UVO-114.PDF

19. Flühs D., Fluhs D., Heintz M., Indenkampen F., Wieczorek C., Kolanoski H. and U. Quast 1996 Direct reading measurement of absorbed dose with plastic scintillators—The general concept and applications to ophthalmic plaque dosimetry. Med. Phys. 23, 427–434.

20. Flühs D., Heintz M., Indenkämpen F., Wieczorek C., Kolanski H., and U. Quast 1996 Direct reading measurement of absorbed dose with plastic scintillators—The general concept and applications to ophthalmic plaque dosimetry. Med. Phys. 23, 427–434.

21. Fontbonne J.M., Iltis G., Ban G., Battala A., Vernhes J. C., Tillier J., Bellaize N., LeBrun C., Tamain B., Mercier K. and J. C. Motin 2002 Scintillating fiber dosimeter for radiation therapy accelerator IEEE Trans. Nucl. Sci. 49, 2223–2227.

22. Frelin A.M., Fontbonne J.M., Ban G., Colin J., Labalme M., Batalla A., Isambert A., Vela A. and T. Leroux 2005 Spectral discrimination of Cerenkov radiation in scintillating dosimeters. Med. Phys. 32, 3000–3006.

23. Hendee W., Rand Ritenour E.R. 2002 Medical Imaging Physics.

24. Heydarian M., Hoban P.W., Beckham W.A., Borchhardt I.M. and Beddoe A.H 1993 Evaluation of a PTW diamond detector for electron beam measurements. Phys. Med. Biol. 38 1035-42.

25. Hoban P.W., Heydarian M., Beckham W.A. and Beddoe AH 1994 Dose rate dependence of a PTW diamanond detector in the dosimetry of a 6MV photon beam. Phys. Med. Biol. 39 1219-1229.

26. J.R. Williams, D.I. Thwaites, Oxford University Press, 1993 Radiotherapy Physics in practice.

27. Johns H.E. and Cunningham J.R. 1983 The Physics of Radiology

28. Khan F. 1984 The Physics of Radiation Therapy

29. Knoll G.F. 1989 Radiation Detection and Measurement

30. Law S.H., Fleming S.C., Suchowerska N., McKenzie D.R., Lin T. Cerenkov Radiation in Potical Fiber Communication. Optical Society of America, 1-55752-830-6.

31. Le´tourneaua D., Pouliot J. and R. Roy 1999 Miniature scintillating detector for small field radiation therapy. Med. Phys. 26, 2555-2561.

32. Low D.A., Harms W.B., Mutic S., Purdy J.A. 1998 A technique for the quantitative evaluation of dose distributions. Med. Phys. 25, 656-661.

33. Laub W.U. and Wong T., 2003 The volume effect of detectors in the dosimetry of small fields used in IMRT. Med. Phys. 30, 341-347.

34. Metcalfe P, Kron T., Hoban P. 1997 The Physics of Radiotherapy X-rays from Linear Accelerators

35. Petric P., Robar J. L. and B. G. Clark 2006 Development and characterization of a tissue equivalent plastic scintillator based dosimetry system. Med. Phys. 33, 96–105.

36. Pain F., Laniece P., Mastrippolito R., Charon Y., Comar D., Leviel V., Pujol J. F. and L. Valentin 2000 SIC, an intracerebral radiosensitive probed for in vivo neuropharmacology investigations in small laboratory animals: Theoretical considerations and physical characteristics. IEEE Trans. Nucl. Sci. 47, 25–32.

37. PerkinElmer Optoelectronics 2008 Emitters and Detectors Catalogue.

38. Polymicro Technologies 2008
http://www.polymicro.com/products/opticalfibers/products_opticalfibers_fv.htm

39. Rosenfeld A.B., Carolan M.G., Kaplan G.I., Allen B.J. Khirvrich V.I. 1995 MOSFET dosimeters: The role of encapsulation on dosimetric characteristics in mixed gamma-neutron and megavoltage x-ray fields. IEEE Tans. Nucl. Sci. 42, 1870-1876.

40. Spieler H. Introduction to Radiation Detectors and Electronics. III. Scintillation Detectors. 1998.

41. Technical Report Series 381, 1987 The Use of Plane-Parallel Ionization Chambers in High-Energy Electron and Photon Beams. an International Code of Practice for Dosimetry. International Atomic Energy Agency, Vienna.

42. Technical Report Series 398, 2000 Absorbed Dose Determination in External Beam Radiotherapy. An International Code of Practice for Dosimetry Based on Standards of Absorbed Dose to Water. International Atomic Energy Agency, Vienna.

43. Thomson I., Thomas R., Berndt L. 1984 Radiation dosimetry with MOS sensors. Radiat. Protect. Dosim. 6, 121-124.

44. Wang Y. 2005 Digital film dosimetry in radiotheraphy and the development of analytical applications software. PhD Thesis.

45. Wells M. M., Mackie T. R., M. B. Podgorsak, M. A. Holmes, N.Papanikolaou, P. J. Reckwerdt, J. Cygler, and J. K. Muehlenkamp 1994 Measurement of the electron dose distribution near inhomogeneities using a plastic scintillation detector. Int. J. Radiat. Oncol., Biol., Phys. 29,1157–116.

46. Williamson J.F., Dempsey J.F., Kirov A.S., Monroe J.I., Binns W. R. and Hedtjärn H. 1999 Plastic scintillator response to low-energy photons Phys. Med. Biol. 44 857-871

47. Wolfram U Laub, Theodor W K and Fridtjof N 1999 A diamond detector in the dosimetry of high-energy electron and photon beams. Phys. Med. Biol. 44 2183-2192.